

WOJCIECH KUZNIK

Quantum-chemical computer simulations
of the linear and non-linear optical
properties of pyrazoloquinoline and
dicyanopyrazine derivatives



TARTU UNIVERSITY PRESS

The dissertation was admitted on March 20, 2012, in partial fulfillment of the requirements for the degree of Doctor of Philosophy in materials science, and allowed for defense by the Scientific Council on Materials Science of the Faculty of Science and Technology of the University of Tartu.

Supervisor: Prof. Mikhail Brik, Institute of Physics, University of Tartu,
Estonia

Opponents: Prof. Bohdan Andriyevskyy, Department Electronics and
Computer Sciences, Koszalin University of Technology

(Ph.D.) Ass. Prof. Mihhail Klopov, Department of Physics,
Faculty of Science, Tallinn University of Technology

Commencement: May 16, 2012 at University of Tartu, Tartu, Estonia

The study was carried out at the Institute of Physics, University of Tartu and Department of Physical Chemistry, Silesian University of Technology, Poland, using resources of Wroclaw Centre for Networking and Supercomputing, grant no. 135. This research was supported by European Social Fund's Doctoral Studies and Internationalisation Programme DoRa.



ISSN 2228-0928

ISBN 978-9949-19-974-7 (trükis)

ISBN 978-9949-19-975-4 (PDF)

Autoriõigus Wojciech Kuznik, 2012

Tartu Ülikooli Kirjastus

www.tyk.ee

Tellimuse nr 173

CONTENTS

CONTENTS	5
LIST OF PUBLICATIONS.....	7
AUTHOR’S CONTRIBUTION.....	8
LIST OF OTHER PUBLICATIONS	9
LIST OF ABBREVIATIONS	11
I. INTRODUCTION.....	12
2. GENERAL BACKGROUND: OBJECTS OF RESEARCH	14
2.1. Structure and application of the studied chromophores.....	14
2.1.1. 1H-pyrazolo[3,4-b]quinoline derivatives	14
2.1.2. Dicyanopyrazine –derived donor- π -acceptor chromophores.....	16
3. METHODS OF CALCULATIONS.....	18
3.1. Introduction	18
3.2. Basic principles and approximations.....	20
3.3. Overview of computational methods.....	22
3.3.1. Molecular Mechanics	22
3.3.2. Semi-empirical methods.....	23
3.3.3. Density Functional Theory	24
3.3.4. TDDFT and CI – theoretical description of excited states	26
3.3.5. Polarizable Continuum Model.....	27
3.3.6. Perturbation theory	28
3.4. Overview of the software used.....	28
3.4.1. Hyperchem 8.04	28
3.4.2. Gaussian 09	29
3.4.3. PCGAMESS/FIREFLY.....	29
3.4.4. GABEDIT	29
4. MODELING OF PYRAZOLOQUINOLINE FLUORODERIVATIVES (I, II).....	30
4.1. Aim.....	30
4.2. Methods.....	30
4.3. Results	31
4.4. Conclusions	39
5. QUANTUM-CHEMICAL DESCRIPTION OF DICYANOPYRAZINE-BASED CHROMOPHORES (III)	41
5.1. Aim.....	41
5.2. Methods.....	42
5.3. Results	43
5.4. Conclusions	47

6. SUMMARY	48
7. SUMMARY IN ESTONIAN	50
8. REFERENCES	52
ACKNOWLEDGEMENTS	54
PUBLICATIONS	55

LIST OF PUBLICATIONS

This thesis is based on the following papers:

- I. M. G. Brik, **W. Kuznik**, E. Gondek, I. V. Kityk, T. Uchacz, P. Szlachcic and B. Jarosz, "Optical absorption measurements and quantum-chemical simulations of optical properties of novel fluoro derivatives of pyrazoloquinoline" *Chemical Physics* **370**, (2010), pp. 194–200
- II. **W. Kuznik**, J. Ebothe, I. V. Kityk, K. J. Plucinski, E. Gondek, P. Szlachcic, T. Uchacz, P. Armatys, "Spectroscopy of fluoroderivatives of 1H-pyrazolo[3,4-b]quinoline in different solvents", *Spectrochimica Acta A* **77** (2010), pp. 130–134
- III. F. Bureš, H. Čermáková, J. Kulhánek, M. Ludwig, **W. Kuznik**, I. V. Kityk, T. Mikysek, and A. Růžicka, "Structure-Property Relationships and Nonlinear Optical Effects in Donor-Substituted Dicyanopyrazine-Derived Push-Pull Chromophores with Enlarged and Varied π -Linkers", *European Journal of Organic Chemistry* **3**, (2012), pp. 529–538

AUTHOR'S CONTRIBUTION

Author's research has given essential contribution to all of the following publications:

Publication I: The author is responsible for the main part of the computer modeling of pyrazoloquinoline flouroderivative chromophores as well as for a part of the analysis of simulation data, preparation of the manuscript and measurement of the absorption spectra.

Publication II: The author performed all the quantum-chemical simulations presented in the article, all spectroscopy experiments and substantially contributed to preparation of the figures and text of the manuscript.

Publication III: The author is responsible for all the quantum-chemical calculations presented in the article as well as for the graphical representation of the experimental and theoretical data and contributed to the text of the manuscript.

LIST OF OTHER PUBLICATIONS

1. T. Kolev, B. Koleva, J. Kasperczyk, Ivan Kityk, S. Tkaczyk, M. Spitel, Ali H. Reshak, **W. Kuźnik** Novel nonlinear optical materials based on dihydropyridine organic chromophore deposited on mica substrate, *Journal of materials Science: Materials in Electronics*, **20**, 11 (2009), pp. 1073–1077.
2. I. Fuks-Janczarek, Ali H. Reshak, **W. Kuźnik**, I. V. Kityk, R. Gabański, M. Łapkowski, R. Motyka, J. Suwiński UV-VIS absorption spectra of 1,4-dialkoxy-2,5bis[2-thien-2-yl]ethenyl]benzenes, *Spectrochimica Acta A*, **72**, 2, (2009), pp. 394–398.
3. **W. Kuźnik**, M. Lemanowicz, A. Kus, M. Gibas, A. Gierczycki, Temperature-controlled particle size distribution of chalk suspension utilizing a thermosensitive polymer, *Powder Technology*, **201**, 1, (2010), pp. 1–6.
4. A. H. Reshak, J. Ebothe, A. Wojciechowski, **W. Kuźnik**, A. Popeda, Optically stimulated non-linear optics effects in semiconducting nanocrystallites, *Physica E* **42**, 5, (2010), pp. 1769–1771.
5. T. Satyanarayana, I. V. Kityk, Y. Gandhi, V. Ravikumar, **W. Kuźnik**, M. Piasecki, M. A. Valente, N. Veeraiah, Optically induced effects in nano-crystallized PbO–Sb₂O₃–B₂O₃:Pr₂O₃ glasses, *Journal of Alloys and Compounds* **500**, 1, (2010), pp. 9–15.
6. El-Naggar, A. M., Alzayed, N. S., Majchrowski, A., Jaroszewicz, L., Brik, M. G., **Kuźnik, W.** & Kityk, I. V. 2011, “Preparation and fluorescence properties of La₂CaB₁₀O₁₉ crystals doped with Pr³⁺ ions”, *Journal of Crystal Growth*, **334**, 1, pp. 122–125.
7. **Kuźnik, W.**, Kityk, I. V., Kopylovich, M. N., Mahmudov, K. T., Ozga, K., Lakshminarayana, G. & Pombeiro, A. J. L. 2011, “Quantum chemical simulations of solvent influence on UV-vis spectra and orbital shapes of azoderivatives of diphenylpropane-1,3-dione”, *Spectrochimica Acta – Part A: Molecular and Biomolecular Spectroscopy*, **78**, 4, pp. 1287–1294.
8. Gąsior, P., Danel, K. S., Matusiewicz, M., Uchacz, T., **Kuźnik, W.**, Piatek, L. & Kityk, A. V. 2011, “DFT/TDDFT study on the electronic structure and spectral properties in annulated analogue of phenyl heteroazulene derivative”, *Materials Chemistry and Physics*, **132**, 2–3, 2012, pp. 330–338
9. Gąsior, P., Danel, K. S., Matusiewicz, M., Uchacz, T., **Kuźnik, W.** & Kityk, A. V. 2011, “DFT/TDDFT Study on the Electronic Structure and Spectral Properties of Diphenyl Azafluoranthene Derivative”, *Journal of Fluorescence*, **22**, 1, pp. 81–91
10. Gąsior, P., Gondek, E., Pokladko-Kowar, M., Danel, K. S., Matusiewicz, M., **Kuźnik, W.** & Kityk, A. V. 2011, “Methoxyphenyl indeno-pyrazoloquinoline derivatives as green fluorescent emitters for polymer based electroluminescent devices”, *Optical Materials*, **34**, 1, pp. 317–321.

11. **Kuznik, W.**, Brik, M. G., Cieřlik, I., Majchrowski, A., Jaroszewicz, L., Alzayed, N. S., El-Naggar, A. M., Sildos, I., Lange, S., Kiisk, V. & Kityk, I.V. 2012, “Changes of fluorescent spectral features after successive rare earth doping of gadolinium oxide powders”, *Journal of Alloys and Compounds*, **511**, 1, pp. 221–225
12. Liu, J., Xu, H., Liu, X., Zhen, Z., **Kuznik, W.** & Kityk, I. V. 2011, “Novel promising crosslinkable tricyanopyrroline polymeric electro-optic materials”, *Journal of Materials Science: Materials in Electronics*, DOI: 10.1007/s10854-011-0569-5

LIST OF ABBREVIATIONS

AM	– Austin Model
CIS	– Configuration Interaction – Singlets
CPHF	– Coupled-Perturbed Hartree-Fock
D- π -A	– Donor- π -linker-Acceptor system
DFT	– Density Functional Theory
HOMO	– Highest Occupied Molecular Orbital
ICT	– Intramolecular Charge Transfer
LED	– light emitting diode
LUMO	– Lowest Occupied Molecular Orbital
MM	– molecular mechanics
NLO	– non-linear optics
OLED	– organic light emitting diode
PCM	– Polarizable Continuum Model
PM	– Parameterized Model
PQ	– 1H-pyrazolo[3,4-b]quinoline
PQF	– a fluorine-containing derivative of 1H-pyrazolo[3,4-b]quinoline
RM	– Recife Model
SCF	– Self-Consistent Field
SHG	– Second Harmonic Generation
TDDFT	– Time-Dependent Density Functional Theory
UV-vis	– Ultra-Violet – visible (light)

I. INTRODUCTION

Search for new optically active materials is one of the most active and rapidly developing directions in contemporary science. Scientific community throughout the world attempts to design new optoelectronic devices such as electroluminescent displays [1], photovoltaic cells and organic light emitting diodes (OLEDs) [2], and optical sensors [3].

Possible applications of newly synthesized material to a large extent are determined by its molecular properties. For example, in the case of LEDs and electroluminescent displays the main role is played by the HOMO (Highest Occupied Molecular Orbital) and LUMO (Lowest Unoccupied Molecular Orbital) energy levels, as well as by the linear absorption coefficients (absorption spectrum). If the material is supposed to be used in the nonlinear-optics (NLO) applications, then the nonlinear parameters, like the second and third order hyperpolarizabilities, play crucial role. Among numerous non-linear materials, organic systems for NLO applications are extensively studied as they can be tailor-synthesized and have strong optical nonlinearities [4].

The design of new optically active materials can be substantially aided by quantum-chemical calculations, which can provide the user with reliable information about the structure, electronic, optical, elastic, and non-linear optical properties of the material in question. With this information, one can explain the observed experimental results, predict certain characteristic features of new compounds and set directions of efficient search for new improved materials. Provided that the computational chemistry is more and more widely applied in all the branches of substance/material design, it is reasonable to expect that its importance will grow alongside computational power available to researchers, which has been growing exponentially in the last decades. As a result, in the molecular calculations a large number of atoms (50 or more) is no longer an issue from the point of view of computational efforts.

Since the optical properties of chemical substances are directly resultant from their molecular structure, the quantum-chemical study can help scientists interpret the experimental data, structure-property relationship in particular. Additionally, examining theoretical predictions of molecular properties of new compounds together with organic chemist's intuition can accelerate search for new materials. Thus, computational chemists frequently cooperate with "traditional" specialists in organic chemistry which often leads to common publications, such as those this thesis comprises of.

Even though exact prediction of molecular parameters such as orbital energies or hyperpolarizabilities are rarely obtained from quantum-chemical simulations, the computational chemistry methods usually successfully reproduce their relative values in a series of compounds [5], as will also be demonstrated in this thesis.

The main aims of the present work were as follows:

- Theoretical description of absorption spectra of new chromophores from pyrazoloquinoline group using three different semi-empirical methods
- Application of quantum-chemical computer simulations to modeling solvent influence on optical properties of fluorine-substituted pyrazoloquinoline derivatives. The chosen method is Time-Dependent Density Functional Theory supplemented with Polarizable Continuum Model of solvation effects.
- Quantum-chemical simulations of new optically active substances from the pyrazine group, including molecular orbital energies, energy gap and dynamic hyperpolarizability in relation to experimental data obtained from electrochemical and non-linear optics experiments.

In all considered cases the quantum-chemically derived results were validated with corresponding experimental data; agreement between them was discussed in details. Computational chemistry methods were shown to be a useful tool in all the cases presented in this work. As such, they can be applied to aid design of new optically active materials with desirable properties.

2. GENERAL BACKGROUND: OBJECTS OF RESEARCH

2.1. Structure and application of the studied chromophores

2.1.1. 1H-pyrazolo[3,4-b]quinoline derivatives

1H-pyrazolo[3,4-b]quinoline is an organic optically active substance containing aromatic moieties of pyrazole and quinoline (Figure 1). For the sake of simplicity it will be abbreviated hereafter PQ. It was first prepared by Tomasik over 80 years ago [6], but optical properties of PQ derivatives were not studied until recently. They are known to exhibit good fluorescent properties with emission ranging from blue to yellow, depending upon the substituents [7, 8] or solvent [9, 10]. PQ derivatives gained considerable attention due to their potential application in optoelectronic devices [11, 12].

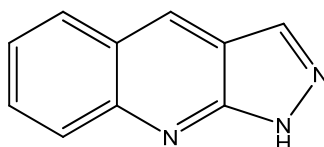


Figure 1. Structure of 1H-pyrazolo[3,4-b]quinoline (PQ).

As side substituents are known to significantly change properties of the PQ chromophores, fluorine-substituted derivatives were chosen for research (Figure 2, Figure 3). It was of particular interest to establish how a small, but strongly electronegative atom influences optical spectra of the new chromophores.

The central part of the PQ molecule is an aromatic moiety with delocalized π -electronic system. Addition of side substituents affects properties as HOMO and LUMO energy levels, the effect depending upon whether the substituent is electron-donating or electron-withdrawing, as well as whether its electronic system can conjugate with the central part leading to further delocalization.

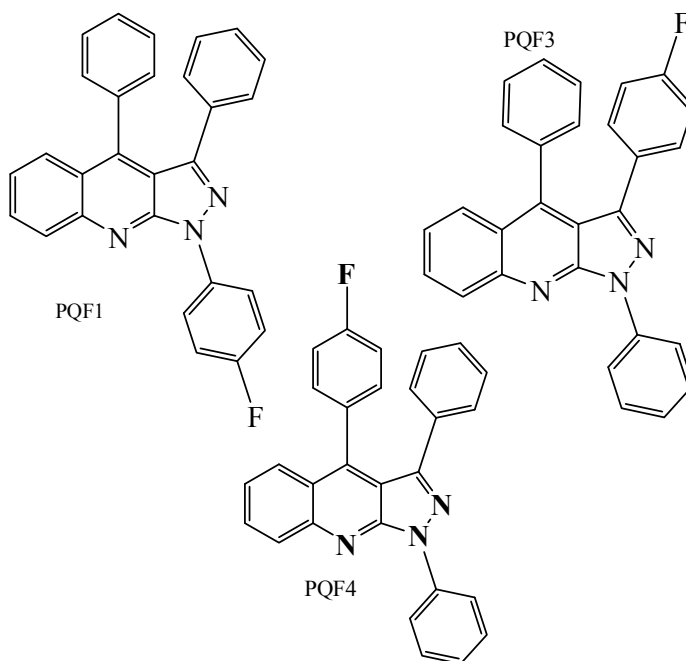


Figure 2. Structural formulae of 1-(4-fluorophenyl)-3,4-diphenyl-1H-pyrazolo[3,4-b]quinoline (PQF1), 3-(4-fluorophenyl)-1,4-diphenyl-1H-pyrazolo[3,4-b]quinoline (PQF3) and 4-(4-fluorophenyl)-1,3-diphenyl-1H-pyrazolo[3,4-b]quinoline (PQF4).

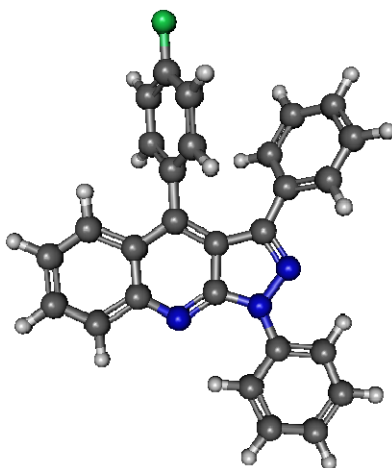


Figure 3. Equilibrium geometry of PQF4. Other PQ derivatives depicted in the thesis differ in F atom position (green).

2.1.2. Dicyanopyrazine – derived donor- π -acceptor chromophores

An organic molecule exhibiting strong NLO properties typically consists of electron donor (D) and electron acceptor group (A) connected by a π -conjugated system, which allows for intramolecular charge transfer between the donor and acceptor moieties. Such structures are often referred to as D- π -A or push-pull systems where acceptor group “pulls” electrons from “pushing” donors through a “ π -corridor” [4]. Nonlinear responses of the chromophores depend upon each of the elements comprising them – acceptors, donors and conjugated linkers [13].

A new set of substances based on pyrazine was chosen for study in search of new NLO-phores. In these molecules (Figure 4) the trimethylamino groups are electron-donating, cyano groups electron-accepting groups and a phenyl rings either conjugated via ethynylene moiety or unconjugated serve as π -linkers.

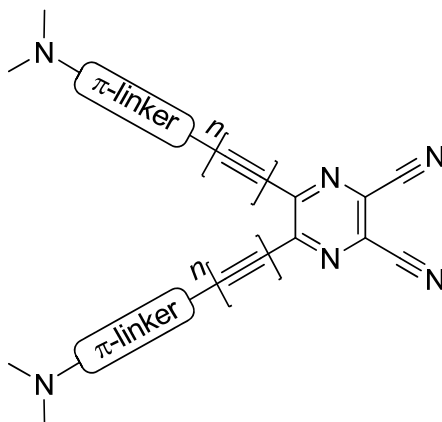


Figure 4. A general structure of a X-shaped pyrazine-based chromophore.

From organic chemists’ intuition and experience it can be predicted that such chromophores are good candidates for Nonlinear Optics (NLO) applications. It is thus crucial that a relationship is established between the D- π -A structure of the NLO-phore and its properties. The computer Coupled-Perturbed Hartree-Fock (CPHF) simulations can help establish this relationship and once proven successful they can aid preparation of new NLO materials at an early design level, which was motivation for the work presented in Publication III.

As depicted in Figure 5 using one of the substances from Publication III as an example, absorption of a quantum of light which induces an electron excitation from Highest Occupied to Lowest Unoccupied Molecular Orbital (HOMO to LUMO) at the same time changes drastically the charge distribution in the molecule.

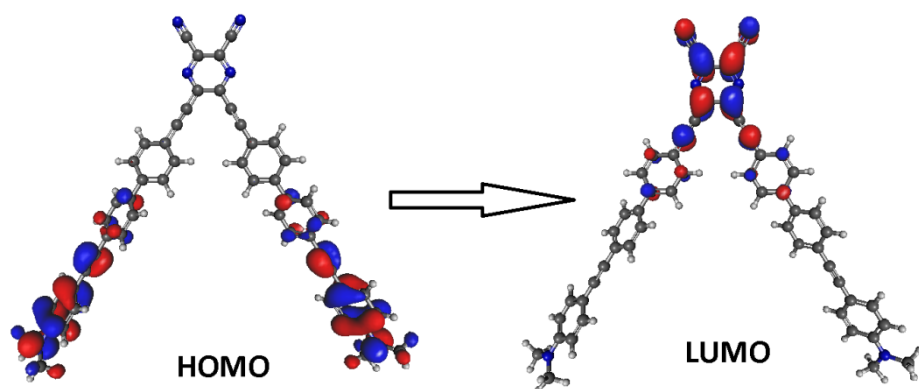


Figure 5. Intermolecular Charge Transfer in one of the studied molecules.

3. METHODS OF CALCULATIONS

3.1. Introduction

Computational chemistry is a branch of theoretical chemistry (or physics) which describes properties of molecules and macromolecular structures by solving appropriate equations using computers. The equations can be based on first principles (*ab initio* methods). The equations solved are then in fact the Schrödinger equation with necessary approximations. They can also be purely empirical (molecular mechanics), in which case a complete set of experimentally derived parameters needs to be known in order to produce useful results. Finally, the approach to the modeling can be intermediate between *ab initio* and empirical: semi-empirical and DFT methods are the most widely used examples. As a general rule the more empirical parameters a method uses, the faster it is, but the less accurate as well, because the simplifications made constrain its ability to describe certain phenomena. The extreme example is Molecular Mechanics, which treats a set of atoms as spherical objects connected by springs; the spheres' radii and spring constants are the empirically derived parameters used. It is extremely fast compared to the *ab initio*, or even semi-empirical methods, but at the same time Molecular Mechanics is incapable of reproducing any molecular properties involving electrons. The *ab initio* methods are, on the contrary, accurate, and virtually all molecular properties can be addressed by them, but at substantially increased computational cost, and as such they cannot be applied to large systems even with the use of supercomputers. For this reason most of the publications published contemporarily use either semi-empirical or DFT methods as a reasonable compromise between model accuracy and computational cost, and so does this thesis. Figure 6 below shows relation between different classes of the quantum chemical computational models and indicates directions of the calculating speed and computational accuracy increase.

Computational chemistry simulations are not only a tool to interpret experimental data. When a correct approach is specified for the studied group of compounds, it is possible to predict properties of a new substance solely by computer simulations. Quantum-chemists are frequently employees of pharmaceutical companies; as such they have to be able to predict which substances are most probable to be effective drugs. Even if they are not always correct in their predictions, just by eliminating the least probable drugs quantum-chemical simulations reduce empirical research which in pharmaceutical industry is extremely expensive and time-consuming.

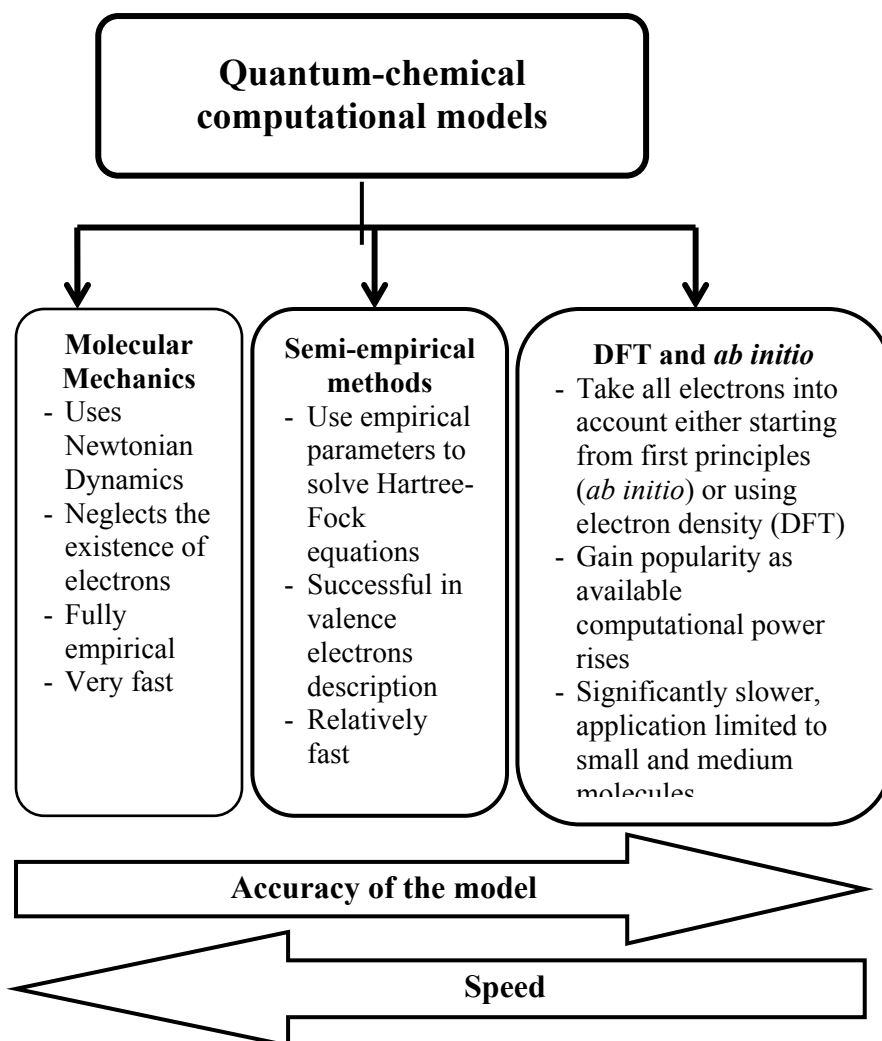


Figure 6. Schematic classification of the main groups of modern quantum-mechanical methods used for description of various properties of molecules.

The theoretically derived results in vast majority of cases need to be at least partially verified experimentally, but the current state of computational chemistry allows to speculate that in the future more and more experimental work will be replaced by simulations. What once was just another science-fiction idea, can soon become reality, just as it has previously happened with airplanes, space travel, mobile (video)phones and last but not least, computers.

A detailed description of computational chemistry methods can be found in many articles [14, 15] and books [16,17] devoted to this subject. As this thesis concentrates on practical applications of computational chemistry methods in

predicting optical properties of the chosen chromophores, and also due to space limitations, this chapter contains only a brief overview of quantum chemistry principles and computational methods used by the author.

The chapter also contains a short description of quantum-chemistry programs used and information about free of charge licensed use of some of them.

3.2. Basic principles and approximations

The basic principle describing quantum systems is the Schrödinger equation:

$$H\Psi_i(R, r) = E_i\Psi_i(R, r) \quad (3.1)$$

Where $\Psi_i(R, r)$ is a wavefunction of the system dependent on both electronic variables (r) and positions of the nuclei (R), H is the energy operator (Hamiltonian) and E_i is the total energy of the system, or the eigenvalue of the H operator. The index i denotes possible solutions of the equation, or, on other words, allowed quantum mechanical states of the system.

The Hamiltonian of the system can be written as:

$$H = -\sum_k \frac{\hbar}{2M_k} \nabla_k^2 - \frac{\hbar}{2m_e} \sum_i \nabla_i^2 + \frac{1}{2} \sum_{k \neq l} \frac{Z_k Z_l e^2}{|R_k - R_l|} + \frac{1}{2} \sum_{i \neq j} \frac{e^2}{|r_i - r_j|} + \sum_{i,k} \frac{Z_i e^2}{|r_i - R_k|} \quad (3.2)$$

where the operators used are the nuclei kinetic energy, electrons kinetic energy and potential energy operators of electrostatic interaction: nucleus-nucleus, electron-electron and electron-nucleus, respectively.

As the masses of the nuclei are several orders of magnitude larger than the mass of an electron, they move very slowly compared to electrons. Thus, they can be regarded motionless, and as a result the Schrödinger equation can be separated with respect to R and r variables. This approach is known as the Born-Oppenheimer approximation [18]. It allows one to separate a system into two subsystems: fast moving electrons and “frozen” nuclei. These subsystems are described by two separate equations, i.e.

nuclear:

$$H^N \phi_N(R) = E^{tot} \phi_N(R) \quad (3.3)$$

$$H^N = -\sum_k \frac{\hbar}{2M_k} \nabla_k^2 + \frac{1}{2} \sum_{k \neq l} \frac{Z_k Z_l e^2}{|R_k - R_l|} + E(R) \quad (3.4)$$

and electronic:

$$H^e \psi_e(R, r) = E^e \psi_e(R, r) \quad (3.5)$$

$$H^e = -\frac{\hbar}{2m_e} \sum_i \nabla_i^2 + \frac{1}{2} \sum_{i \neq j} \frac{Z_i e^2}{|r_i - r_j|} + \sum_{i,k} \frac{e^2}{|r_i - R_k|} \quad (3.6)$$

in which R is a parameter, not a variable. The wave functions ϕ_N and ψ_e are called the nuclear and electronic wavefunctions, respectively. The nuclear Hamiltonian also includes electronic system energy dependent on nuclear positions $E(R)$ which is a constant value for any defined set of nuclear positions. As the Born-Oppenheimer energies must be equivalent to the total energy of the system, the Ψ wavefunction can be treated as a product of the ϕ_N and ψ_e :

$$\Psi \approx \phi_N(R) \psi_e(R, r) \quad (3.7)$$

If this wavefunction is introduced into the Schrödinger equation

$$H \phi_N(R) \psi_e(R, r) = E \phi_N(R) \psi_e(R, r) \quad (3.8)$$

And integrated over electronic coordinates, it yields an equation describing the movement of the nuclei:

$$\left[\frac{\hbar}{2\mu} \Delta_R + E_{adN} + E_e(R) \right] \phi_N(R) = E \phi_N(R) \quad (3.9)$$

Where Δ_R is the Laplacian operator acting upon the nuclear coordinates, $E_e(R)$ is the electronic energy of a particular nuclear positions and E_{adN} is an average value of nuclear kinetic energy operator.

$$E_{adN}(R) = \int \psi_e^* T_N \psi_e d\tau \ll E_e(R) \quad (3.10)$$

Omitting E_{adN} yields the Born-Oppenheimer approximation. It gives reasonable solutions of the Schrödinger equation only for systems containing several electrons. Practical applications of computational chemistry require another approximation: the Hartree-Fock approach. The multi-electron wavefunction for a system of N electrons is assumed to be a product of single electron wavefunctions called a spin-orbital:

$$\psi_e = \varphi_1(1) \varphi_2(2) \varphi_3(3) \dots \varphi_N(N) \quad (3.11)$$

Each electron in the system is described by a spin-orbital which is a function of the spin (α, β) and spatial coordinates (ϕ_i): $\psi_e = \phi(r) \sigma(s), \sigma = \alpha, \beta$. There is no interaction between spin-orbitals assigned to identical (impossible to distinguish) electrons. In order to satisfy all the mathematical requirements for an electron-describing wavefunction, it is convenient to define it as a determinant of a matrix:

$$\psi_e = \frac{1}{\sqrt{N!}} \begin{bmatrix} \phi_1(1) & \phi_1(2) & \cdots & \phi_1(N) \\ \phi_2(1) & \phi_2(2) & \cdots & \phi_2(N) \\ \vdots & \vdots & \ddots & \vdots \\ \phi_N(1) & \phi_N(2) & \cdots & \phi_N(N) \end{bmatrix} \quad (3.12)$$

The coefficient $1/\sqrt{N!}$ is a normalization coefficient, ensuring that the sum of all electrons in an N-electron system is equal to N. Such a form of representation of the many-electrons wavefunction is known as the Slater determinant. It automatically satisfies the Pauli exclusion principle, which forbids two or more electrons have identical sets of quantum numbers (is a square matrix has two identical columns, its determinant – and the wave function in the above representations – is equal to zero).

In principle, instead of solving the interaction equations between each pair of electrons, each electron is considered to be placed into the effective potential created by the nucleus and the remaining (N-1) electrons. Once the effect of the electron field is included in the electron's description, the algorithm moves to the next one (which is in effective potential of all other electrons, including the one changed in the previous step) and the iterative process continues until convergence is achieved, i.e. the electrons form Self Consistent Field (SCF).

3.3. Overview of computational methods

3.3.1. Molecular Mechanics

Molecular Mechanics is a purely empirical approach to molecular systems. It treats atoms as material spheres and chemical bonds as “springs” connecting them. It relies on a set of empirical parameters including sphere radius, atom mass, “spring” equilibrium length and constant. The calculations are based on Newtonian dynamics and Hooke's law.

A short summary of the main assumptions of Molecular Mechanics can be given as follows:

- each atom is represented as a single sphere with a certain radius (van der Waals radius, for example), polarizability and electric charge (which can be either obtained from chemical formula, or considered as an additional parameter);
- distance between the atoms is considered to vary around the equilibrium (calculated or experimental) bond length;
- interactions between atoms are described by the Hooke's law; as such, knowledge of force constants is required for each type of atomic pairs in a molecule;
- only interaction with the nearest neighbors is considered.

Molecular Mechanics has one main advantage: computational speed. It is extremely fast compared even to semi-empirical methods, not to mention DFT

or *ab initio*. It has, however, a number of disadvantages. Even though it is able to produce good approximation of equilibrium geometry (when electron-electron interactions are not playing significant role), its applications remain limited and as an over-simplified model it does not give a deep insight into many molecular properties. As the model does not even acknowledge existence of electrons, it is not able to produce any electron-related results, and it fails to properly optimize equilibrium geometries of molecules containing π -electron subsystems, sometimes twisting aromatic rings out of planarity*. Nonetheless, Molecular Mechanics model with MM+ force field [19] was used in geometry optimization in Publication I as it had been reported to yield a reasonably good results for similar systems in the past [20]. In many cases Molecular Mechanics owing to its speed remains the only reasonable choice of computational method, for example for systems comprised of thousands of atoms or molecular dynamics, where other methods would not produce any results in an acceptable timeframe.

3.3.2. Semi-empirical methods

Semi-empirical methods treat studied systems with Hartree-Fock formalism, but involve many approximations by the use of empirical parameters[†]. This enables a cost-efficient treatment of electron correlation effects, but at the same time the results obtained depend on how similar the studied system is to the reference molecules which were used to derive the empirical parameters. The two-electron terms of Hamiltonian are not treated explicitly by semi-empirical methods. Instead, the Hückel [21, 22] and extended Hückel [23] approaches are used for π -electrons and valence electrons, respectively.

Currently, the most widely used semi-empirical methods are AM1 [24] and PM3 [25], a newer RM1 [26] method was used in this thesis as well.

The AM1 method (Austin Model) is based on earlier MNDO (Modified Neglect of Differential Overlap) methods [27,28], but uses improved parametrization system for better description of atomic repulsion. Instead of 7 (MNDO), it uses from 13 to 16 empirical parameters per atom.

RM1 (Recife Model 1) is essentially identical to AM1, but it uses an optimized set of parameters. Even though has been reported to yield better results [26], its efficiency in practical uses must yet be confirmed by larger number of researchers.

PM3 (Parameterized Model) is closely related to AM1 as well. They differ in description of core repulsion and in parameter set used.

* Aromaticity is included implicitly, in larger force constants of aromatic bonds (“springs”), but this only limits the twist out of planarity and does not eliminate it

[†] In fact, „empirical” parameters are sometimes derived from *ab initio* calculations, especially where experimental data was not available

Semi-empirical methods are frequently a method of choice in quantum-chemical calculations as they are considered to be a fair compromise between calculation accuracy and computational time. It is very difficult to choose *a priori* the mostly suitable method of calculations; therefore, it is wise to use several different models to get more confidence in the obtained results.

3.3.3. Density Functional Theory

Differential Functional Theory (DFT) is a widely used branch of quantum-chemical methods which is based on Hohenberg-Kohn theorems [29,30]:

In simplistic form the first theorem states that the ground state energy from the Schrödinger equation is a unique functional of the electron density:

$$\rho(\mathbf{r}) = 2 \sum_{i=1}^N \psi_i^*(\mathbf{r}) \psi_i(\mathbf{r}) \quad (3.13)$$

which is expressed in terms of the one-electron wave functions $\psi_i(\mathbf{r})$. The pre-multiplier of 2 appears in front of the summation sign because of the electron's spin. Another way of stating the same theorem is to say that the ground-state electron density uniquely determines all properties of a ground state, including its energy and wave function. An essential result of this theorem is that it allows to reduce finding solution of the Schrödinger equation with 3N variables to simply finding a suitable function of three spatial variable, which describe the electron density distribution, and which then, by virtue of the first Hohenberg-Kohn theorem, will provide exact description of the system's ground state.

At the same time, the first Hohenberg-Kohn theorem postulating existence of the electron density functional says nothing about what this functional looks like. This is the second Hohenberg-Kohn theorem, which gives a key to the choice of the electron density functional: the electron density that minimizes the energy of the overall functional is the true electron density corresponding to the full solution of the Schrödinger equation.

If the "true" functional were known, the electron density could be varied until reaching the energy minimum. This variational principle forms the key stone of application of these two theorems. The energy functional can be written as

$$E[\psi_i] = E_{\text{known}}[\psi_i] + E_{\text{XC}}[\psi_i] \quad (3.14)$$

where ψ_i is the one-electron wave function, the first term in the right-hand side represents all "known" terms (given by Eq. (3.2)) and all everything else is hidden in the second term of the right-hand side, also known as the exchange-correlation functional.

Kohn and Sham have shown that the right electron density can be found by solving a set of the one-electron equations, each of which involves only one electron and is very similar to the Schrödinger equation:

$$\left[-\frac{\hbar^2}{2m} \nabla^2 + V(\mathbf{r}) + V_H(\mathbf{r}) + V_{xc}(\mathbf{r}) \right] \psi_i(\mathbf{r}) = \varepsilon_i \psi_i(\mathbf{r}) \quad (3.15)$$

with

$$V_H(\mathbf{r}) = e^2 \int \frac{\rho(\mathbf{r}')}{|\mathbf{r} - \mathbf{r}'|} d^3 \mathbf{r}' \quad (3.16)$$

being the Hartree potential. It describes the Coulomb repulsion between that electron which is considered in one of the Kohn-Sham equations and the total electron density defined by all electrons in the system. It also incorporates the so-called self-interaction, because the considered electron also contributes to the formation of the total electron density. Therefore, it describes, in other words, the Coulomb interaction between the electron and itself, which is an unphysical interaction, of course. The correction for such an unphysical interaction is also included into the exchange-correlation potential $V_{xc}(\mathbf{r})$, which is defined as the functional derivative of the exchange-correlation energy

$$V_{xc}(\mathbf{r}) = \frac{\delta E_{xc}(\mathbf{r})}{\delta \rho(\mathbf{r})} \quad (3.17)$$

Here the functional derivative (which, strictly speaking, is not equal to the functions's derivative) is shown by symbol δ .

It can be seen that the electron density $\rho(\mathbf{r})$ enters the Hartree potential. At the same time, it is a key-variable to determine the exchange-correlation potential $V_{xc}(\mathbf{r})$. To find an exit from this locked circle, the following algorithm is applied:

1. An initial (trial) electron density $\rho(\mathbf{r})$ is defined. It can be a “good guess” or an already known density for a similar system.
2. The Kohn-Sham equations are solved with this trial density to find the single-electron wave functions $\psi_i(\mathbf{r})$.
3. The electron density $\rho(\mathbf{r})$ is calculated with *those* $\psi_i(\mathbf{r})$.
4. The calculated in step 3 electron density is compared with that one used in step 1. If these two densities are identical, the ground state electron density is found and it can be used to calculate the total energy of a system etc. If these two densities are different, than the trial density should be updated and the whole procedure is repeated until the difference between the two electron densities from two consecutive iteration procedures will not exceed an earlier chosen accuracy limit.

3.3.4. TDDFT and CI – theoretical description of excited states

All the methods described previously are applicable to the ground state only. However, the knowledge of the excited states properties is of paramount importance when analyzing the luminescence spectra and potential perspectives of a given material to be a good phosphor, for example. In order to describe excited states, computational chemists usually use Configuration Interaction (CI) or Time-Dependent DFT (TDDFT).

Approximation of a wave function with Slater determinant does not take into account correlation effects and as a consequence fails to properly describe excited states. In CI method the Slater determinant is formed with a number of the spin-orbitals exceeding the number of electrons in the system. The unoccupied orbitals are called virtual. The correlation effects are included by mixing the occupied and virtual states, with wave function defined as follows:

$$\begin{aligned} \psi^{CI} = & d_0 \psi_0 + \sum_{a=1}^{\frac{n}{2}} \sum_{x=\left(\frac{n}{2}\right)+1}^s d_{ax} \psi_{\frac{a}{x}} + \\ & \sum_{a=1}^{\frac{n}{2}} \sum_{b=1}^{\frac{n}{2}} \sum_{x=\left(\frac{n}{2}\right)+1}^s \sum_{y=\left(\frac{n}{2}\right)+1}^s d_{abxy} \psi_{\frac{ab}{xy}} + \dots \end{aligned} \quad (3.18)$$

Where a and b are the occupied and x and y are the virtual orbitals. The first term is the ground state, the second term corresponds to the single-electron transitions and the third one is related to the two-electron transitions. Once the virtual orbitals are known, excited states and optical transitions can be established. The correlation effects are included by CI at a cost of increased computational requirements. The wave function and energy depend on the number of excited states taken into account, and the large number of determinants causes slow convergence.

TDDFT [31] is used for description of excited states, and as such can be employed in a wide range of applications, especially in simulation of new optically active compounds. It is based on the fact that frequency-dependent polarizability $\alpha(\omega)$ describes the response of the dipole moment to an electric field changing in time with frequency $\omega(t)$:

$$\alpha(\omega) = \sum_{\text{exc}} \frac{f_{\text{exc}}}{\omega_{\text{exc}}^2 - \omega^2} \quad (3.19)$$

where ω_{exc} denotes the excitation energy and the sum runs over all excited states. It can be immediately seen that when $\omega_{\text{exc}} = \omega$ (resonance condition) the dynamic polarizability raises to infinity. The residues f_{exc} correspond to the oscillator strengths and together with the excitation energies can be used to construct electronic absorption spectrum which usually lies in the UV-vis range.

3.3.5. Polarizable Continuum Model

Polarizable Continuum Model (PCM) [32,33] is a solvation model frequently used in computational chemistry. If the solvent molecules were to be treated explicitly, they would give tremendous rise to processor and memory demands of quantum-chemical simulations. Instead, PCM regards the solvent as a uniform, continuous space filled with dielectric medium. It requires dielectric constant to be included in the simulation input, to characterize the solvent properties. The parameters for most common solvents are included in packages like Gaussian or FIREFLY and can be invoked by an appropriate keyword as extension for DFT and TDDFT calculation [34]. The model calculates free energy of the molecule as sum of the dispersion-repulsion (dr) and electrostatic (el) interactions and the energy of cavitation (cav):

$$G_{\text{sol}} = G_{\text{dr}} + G_{\text{el}} + G_{\text{cav}} \quad (3.20)$$

In PCM the molecule is placed in a cavity created by intersecting spheres, each sphere centered on atomic nucleus. The point charges placed on the surface created by the overlapping spheres define the solvent reaction field (Figure 7). The reaction field is rendered self-consistent with the solute molecule's electrostatic potential in an iterative procedure, thus yielding the energy in solution.

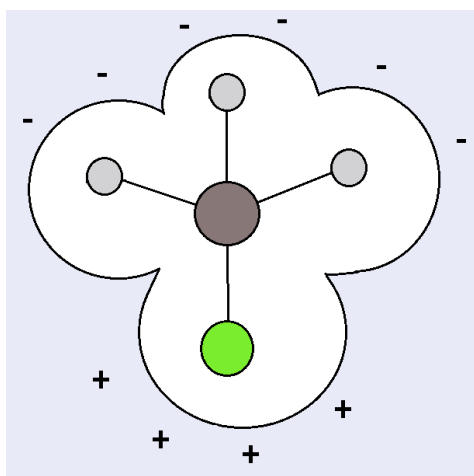


Figure 7. A schematic representation of PCM principle. The molecule is surrounded by a continuous dielectric medium. Point charges are induced by the molecule on the solvent accessible surface formed by atom-centered, overlapping spheres. The surface charges induce changes in the molecule and the whole process is iteratively repeated until the interactions acquire equilibrium

3.3.6. Perturbation theory

In principle, electromagnetic field influencing the molecule is treated as a perturbation affecting the unperturbed molecule's Hamiltonian H_0 :

$$H = H_0 + \lambda H_1 \quad (3.21)$$

Where $\lambda \in < 0, 1 >$ denotes a parameter used to ensure the perturbation is taken into account smoothly. Consequently, the energy of the system perturbed by an external field can be represented by a Taylor series expansion around the unperturbed system:

$$E(\lambda) = E_0 + \lambda E^{(1)} + \lambda^2 E^{(2)} + \dots \quad (3.22)$$

Where the $E^{(n)}$ represents the n-th derivative of the energy with respect to the perturbation:

$$E^{(n)} = \frac{1}{n!} \frac{d^n E(\lambda)}{d\lambda^n} \quad (3.23)$$

Different derivatives of the energy represent measurable properties of the described system, such as hyperpolarizabilities.

The computational algorithms to obtain the values of $E^{(n)}$ are well established. For example, Coupled-Perturbed Hartree-Fock (CPHF) equations [35, 36] can be solved numerically in order to produce derivatives of molecular orbital coefficients and as a result the molecule's response to electromagnetic radiation, *i.e.* dynamic hyperpolarizabilities [37,38].

3.4. Overview of the software used

The software used in research hereby presented was carried out with the software briefly described below. It is noteworthy that two of these programs: FIREFLY and GABEDIT are free-of-charge in academic use. As they can be used jointly for both data manipulation and the calculations themselves, anyone can start quantum-chemical aided research at their convenience and without additional costs involved.

3.4.1. Hyperchem 8.04

Hyperchem 8.04 [39] is a commercial quantum-chemical program comprising of molecular mechanics, semi-empirical, DFT and *ab initio* modules. The program also contains in-built intuitive graphical user interface allowing for quick drawing of studied molecules.

3.4.2. Gaussian 09

Gaussian 09 [40] is a popular commercial computational chemistry code. It is capable of performing quantum-chemical simulations at semi-empirical, DFT and *ab initio* levels of theory. Excited states can be simulated by time-dependent or Configuration Interaction [41,42] approaches. The program includes numerous modules addressing more specific research requirements. PCM is readily evoked when solvation effects are to be taken into account, for instance.

3.4.3. PCGAMESS/FIREFLY

Firefly [43], formerly known as PCGAMESS, is a quantum chemistry program partially based on the GAMESS (US) [44] source code. Its capabilities are almost identical to those of Gaussian package, sometimes even exceeding it, for example it can directly calculate third order dynamic hyperpolarizability, while Gaussian cannot. Firefly is free-of-charge in academic use and as such it can present an excellent opportunity to explore quantum-chemistry with budget limitations. It is, however, less popular than Gaussian and the literature, workshops and tutorials are not so easily available as in the case of its commercial counterpart.

3.4.4. GABEDIT

Both the aforementioned programs accept input in the form of a text file with specific composition. The computational details are introduced by keywords and molecular geometry as a set of coordinates. It is virtually impossible to prepare such file without additional software. GABEDIT [45] is a graphical user interface for input preparation and output interpretation. It is capable of preparing calculations for several different programs, including FIREFLY and Gaussian 09, and preparing a graphical interpretation of simulation results. It can be used to visualize molecular orbitals, electron and spin densities, plot UV-vis, IR, Raman and NMR spectra, animations of molecular oscillations assigned to IR signals and much more. It is also convenient to researchers using different computational codes, because it can load geometry optimized in one program and use it to prepare input for another one. It should also be noted that GABEDIT is free of charge in both academic and commercial use.

4. MODELING OF PYRAZOLOQUINOLINE FLUORODERIVATIVES (I, II)

4.1. Aim

Pyrazoloquinoline derivatives are known to be good luminophores [7, 8] with potential application in LED manufacture. In design of such materials it is imperative to prepare a molecule with desirable HOMO and LUMO levels. Description of the orbital energy levels as well as UV-vis absorption spectra with semi-empirical computer simulations was the aim of Publication I.

In practical applications a chromophore is never used in its pure form, but always embedded into an external matrix (with the exception of chromophores bonded to the matrix, like chromophore-containing polymers). The matrix interacts with the incorporated substances changing their structure and properties. Usually these changes are subtle, but in many cases can be quite vivid. Simulation of matrix influence with TDDFT/PCM on absorption spectra of pyrazoloquinoline fluoroderivatives was the aim of publication II.

4.2. Methods

In publication I three semi-empirical methods were chosen to simulate energy levels and UV-vis absorption spectra, namely AM1, PM3 and new RM1 method [26] whose effectiveness was checked with comparison to the former two. The equilibrium geometry of the chromophores was established using Molecular Mechanics. The side substituents do not exert torsional forces on the central aromatic part and thus the limitations of MM+ did not lead to defects in aromaticity in a subsequent semi-empirical calculations. The choice of the aforementioned methods was strongly affected by available computational power – they were all performed on a personal, single-processor computer.

Computational power available during the preparation of Publication III was significantly greater, 8-processor nodes optimized for quantum-chemical calculations at Wrocław Centre for Networking and Supercomputing were used to perform the simulations at DFT level of theory. All the calculations were performed with B3LYP/6-31G basis set. As the equilibrium geometry is influenced by the solvent, in all the cases the geometry was optimized with PCM-modeled solvation, and excited states were simulated in a subsequent TDDFT run also including the solvation model. Four common solvents differing in polarity were chosen as model matrices, namely cyclohexane, dichloromethane, methanol and acetonitrile, listed from the least to the most polar. This enabled easy experimental confirmation of the theoretical model with the use of UV-vis absorption spectra recorded in these solvents.

The experimental IR spectra were recorded in thin film using BIORAD FTS 175 spectrophotometer and compared subsequently with the results of the quantum-chemical simulations.

4.3. Results

All the quantum-chemical calculations must involve correct, or at least approximate, molecular structure of the studied substance. In some cases the molecular geometry is available from experimental data (crystallography), but in majority of cases has to be established in a separate optimization calculations prior to molecular property evaluation. Whether or not the simulated geometry is correct can be partially verified for example by comparison of theoretical and experimental IR spectrum. The signals in IR spectra are optical manifestation of oscillations, rotations and vibrations of atoms and group of atoms in the molecule. It is unlikely that two significantly different conformations of the molecule would have identical IR spectra, so good agreement between theory and experiment is a reliable indicator of correct molecular geometry used in quantum-chemical simulation.

In the case of BLYP/6-31G optimized geometries, the agreement between experimental and theoretically-derived IR spectra is rather good. Starting from a band at around 3000 cm^{-1} , through a distinct signal around 1500 to several peaks in the so-called “fingerprint region”^{*} of the IR spectrum (up to 400 cm^{-1}), there is rather good agreement between the two plots (Figure 8). Additionally, quantum-chemical simulations can be used to aid the spectrum interpretation by facile identification of the oscillations represented by particular signal. As an example, the strongest signal present in theoretical IR spectrum of PQF1 at 1509 cm^{-1} is visualized in Figure 9.

^{*} Spectral signals in this region are characteristic for each substance and thus it can be used to identify the substance, provided the spectrum is already in the database. It is extensively used in criminology.

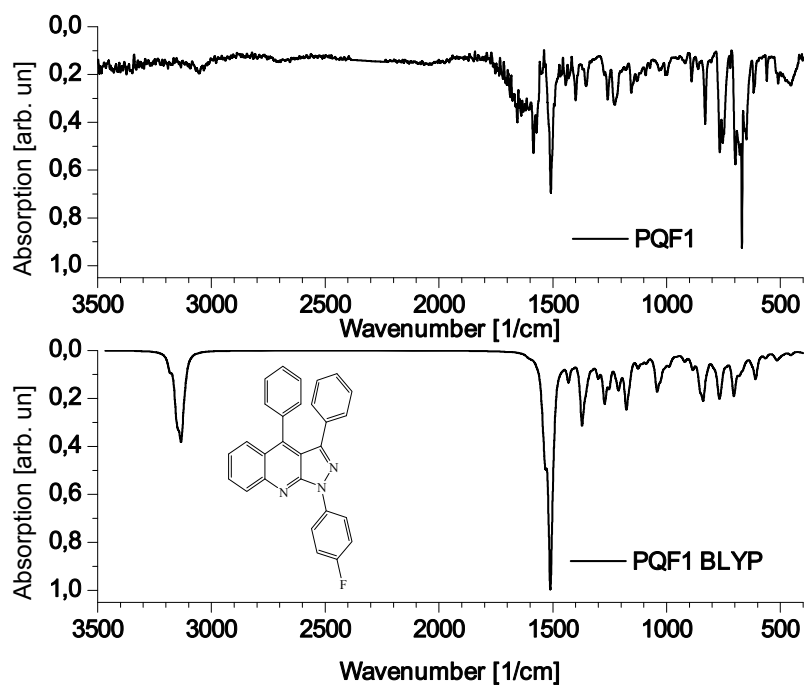


Figure 8. Experimental (top panel) and BLYP/6-31G derived IR spectrum of PQF1.

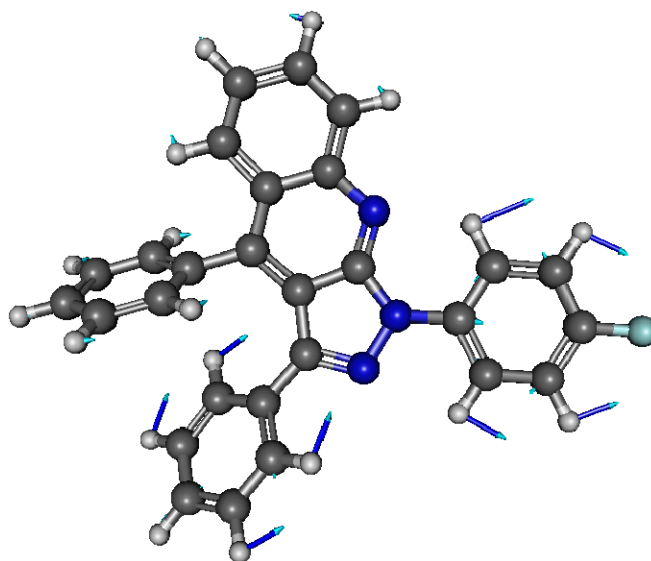


Figure 9. Graphical representation of the most distinctive signal in IR spectrum of PQF1 at 1509 cm^{-1} . The thin blue vector arrows indicate atom movements at this frequency.

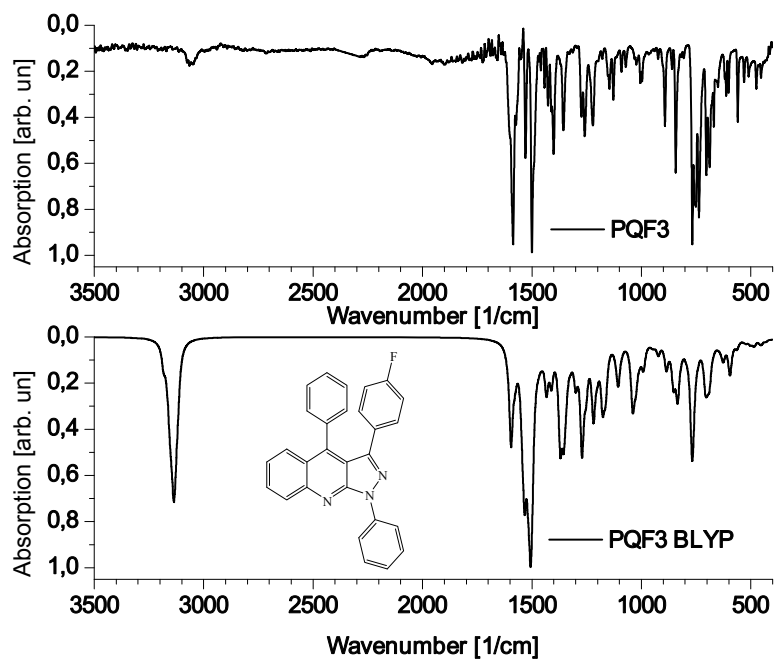


Figure 10. Experimental (top panel) and BLYP/6-31G derived IR spectrum of PQF3.

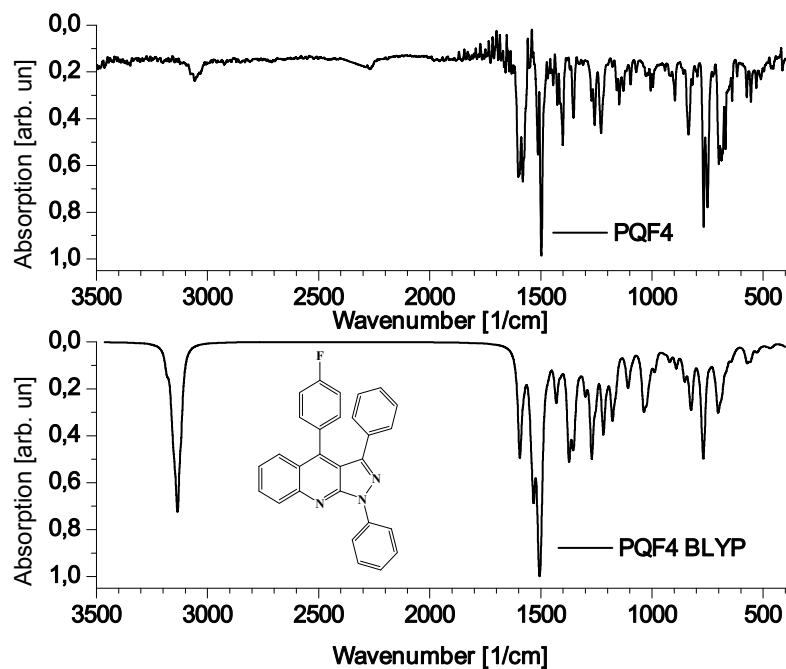


Figure 11. Experimental (top panel) and BLYP/6-31G derived IR spectrum of PQF4.

Configuration Interaction calculations using three different semi-empirical methods, namely PM3, AM1 and RM1, have been performed to produce a reliable description of excited states and plot theoretical UV-vis spectra. In general experimental spectrum resembles the theoretical prediction in terms of transition energies and intensities (Figure 12). It must be noted that the RM1 method and its predecessor, AM1, performed better at predicting the energy gap than the PM3 method. The accuracy of absorption spectra and energy gap prediction was similar to that of much more computationally demanding DFT methods, as can be seen in Table 3.

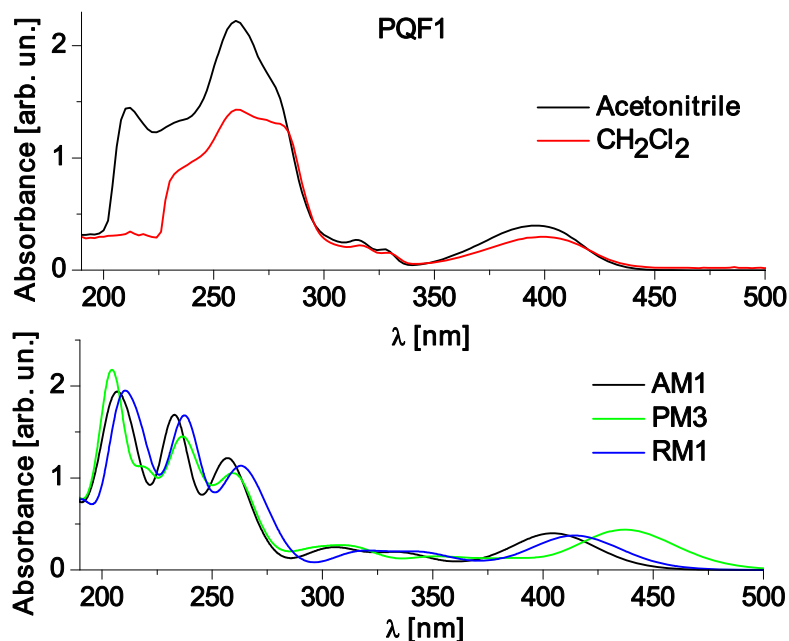


Figure 12. Experimental (top panel) and theoretical (bottom panel) UV-vis spectra of PQF1. The theoretical data was derived via CI calculation at semi-empirical level.

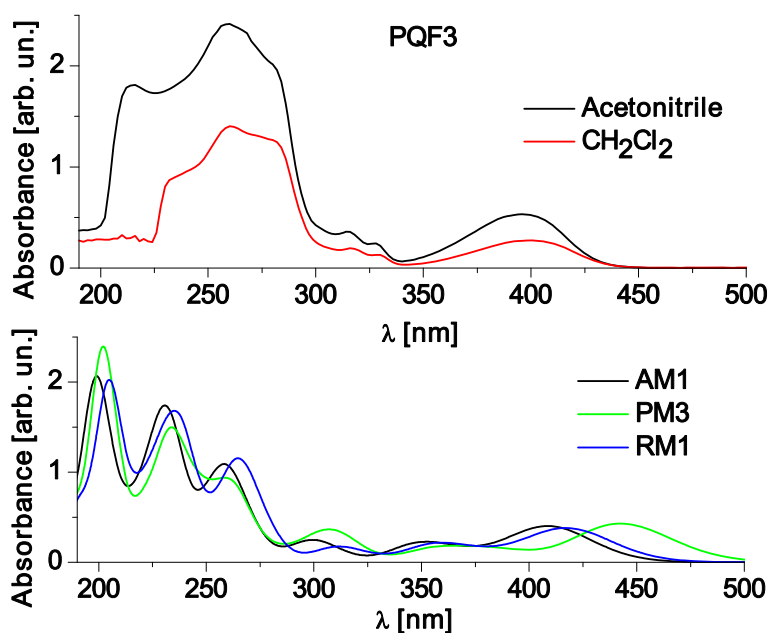


Figure 13. Experimental (top panel) and theoretical (bottom panel) UV-vis spectra of PQF3. The theoretical data was derived via CI calculation at semi-empirical level.

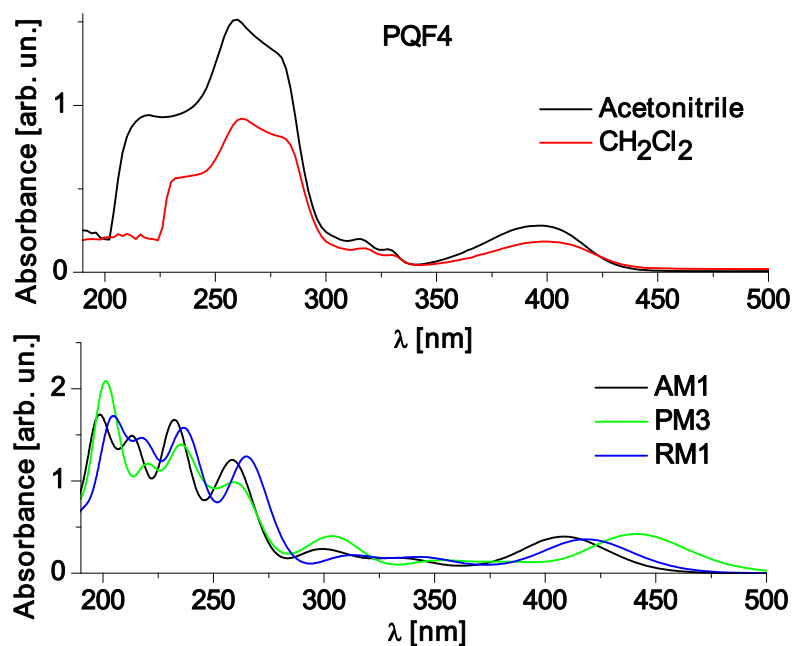


Figure 14. Experimental (top panel) and theoretical (bottom panel) UV-vis spectra of PQF4. The theoretical data was derived via CI calculation at semi-empirical level.

Four solvents were chosen as representative matrices for PQ fluoroderivatives differing in polarity: cyclohexane, dichloromethane, methanol and acetonitrile, listed from nonpolar to polar. The molecular geometries were only slightly changed by the solvents, but the charge distribution along the simulated system was significantly influenced by interaction with the solvent, as demonstrated by the change in dipole moment of the molecule (Table 1). In all the cases the more polar the solvent is, the higher the molecular dipole moment will be. When no solvation model is implemented, the dipole moment is even smaller, demonstrating clearly that solvation effects can play important role in molecular properties. Evidently, the interaction of the molecules with point charges placed at the dielectric medium surface in the PCM model facilitated larger charge separation and, as a result, molecular dipole moment. To demonstrate the difference in charge distribution Mulliken population on fluorine atom is presented in Table 2. The description of charge distribution by Mulliken population analysis is not quantitative, but it is well justified to use it for qualitative comparison [46]. The data in Table 2 is consistent with dipole moments of the PQF equilibrium geometries. In all the cases fluorine atom is a negatively charged moiety at the peripheries of the molecule, thus increase of its charge directly raises the dipole moment, as demonstrated on the example of PQF3 (Figure 15). It is noteworthy, as can be seen in the figure, that change in geometry itself is negligible.

Table 1. Dependence of the dipole moment of PQF molecules on the solvent used in DFT/6-31G/PCM optimization.

Dipole moment [Debye], DFT B3LYP/ 6-31G	Without PCM	Cyclohexane	CH ₂ Cl ₂	CH ₃ OH	Acetonitrile
PQF1	6.1	6.4	7.2	7.4	7.4
PQF3	3.5	3.9	4.5	4.6	4.6
PQF4	1.89	2.4	3.0	3.2	3.2

Table 2. Influence of PCM solvation on Mulliken charge on fluorine atom in B3LYP/6-31G equilibrium geometries of PQF molecules.

Mulliken charge on F atom	Without PCM	Cyclohexane	CH ₂ Cl ₂	CH ₃ OH	Acetonitrile
PQF1	−0.303	−0.309	−0.315	−0.317	−0.317
PQF3	−0.299	−0.306	−0.311	−0.312	−0.312
PQF4	−0.295	−0.302	−0.309	−0.310	−0.310

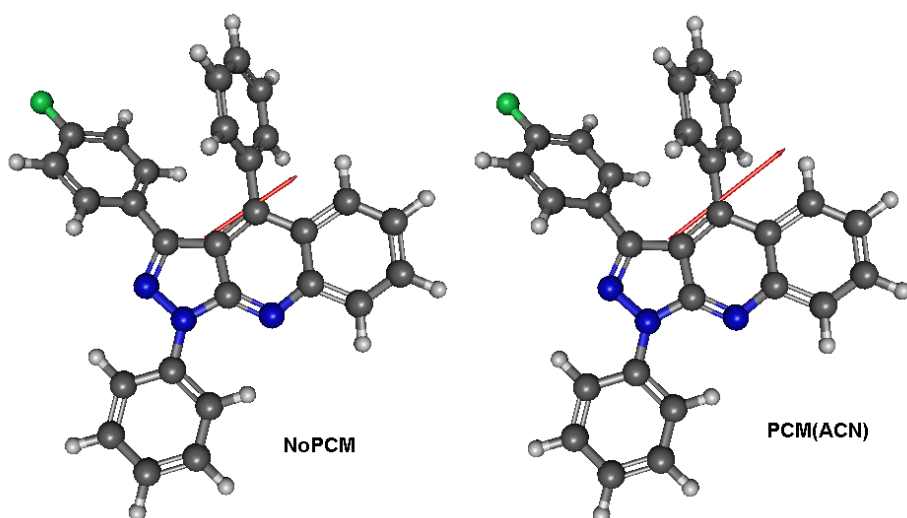


Figure 15. Influence of solvation model on dipole moment of PQF3 (red vectors) which rises from 3.5 to 4.6 D when a PCM solvation in acetonitrile is taken into account in the simulation.

Table 3. Summary of theoretical HOMO, LUMO and Energy Gap values.

Energy [eV], DFT B3LYP/6-31G	Without PCM	Cyclo- hexane	CH ₂ Cl ₂	CH ₃ OH	Aceto- nitrile	AM1	PM3	RM1
PQF1 HOMO	-4.64	-4.70	-4.80	-4.82	-4.82	-8.16	-7.94	-8.06
PQF1 LUMO	-2.54	-2.56	-2.58	-2.60	-2.60	-1.23	-1.40	-1.19
PQF1 Eg (HOMO-LUMO)	2.09	2.13	2.21	2.22	2.22	6.92	6.54	6.87
PQF1 Eg (TDDFT or CIS)	2.88	2.86	2.88	2.89	2.89	3.06	2.84	2.99
PQF3 HOMO	-4.64	-4.71	-4.79	-4.82	-4.82	-8.14	-7.94	-8.06
PQF3 LUMO	-2.54	-2.54	-2.58	-2.60	-2.60	-1.24	-1.41	-1.20
PQF3 Eg (HOMO-LUMO)	2.10	2.17	2.21	2.22	2.22	6.90	6.54	6.86
PQF3 Eg (TDDFT or CIS)	2.86	2.84	2.86	2.87	2.87	3.05	2.84	2.99
PQF4 HOMO	-4.64	-4.70	-4.78	-4.81	-4.81	-8.15	-7.94	-8.06
PQF4 LUMO	-2.55	-2.57	-2.61	-2.63	-2.63	-1.27	-1.43	-1.24
PQF4 Eg (HOMO-LUMO)	2.09	2.12	2.17	2.18	2.18	6.88	6.51	6.82
PQF4 Eg (TDDFT or CIS)	2.84	2.82	2.84	2.85	2.85	3.03	2.81	2.96

The UV-vis absorption spectra of the PQ fluoro derivatives show solvatochromic behaviour. It was possible to reproduce this effect in computer simulations of these materials by implementation of the PCM solvation model. Even though the solvent influence on the absorption bands is rather small (approximately 5 nm blue shift in the first peak maximum in polar methanol with respect to non-polar cyclohexane), a shift of similar magnitude can be observed in the TDDFT-derived spectra (Figure 16).

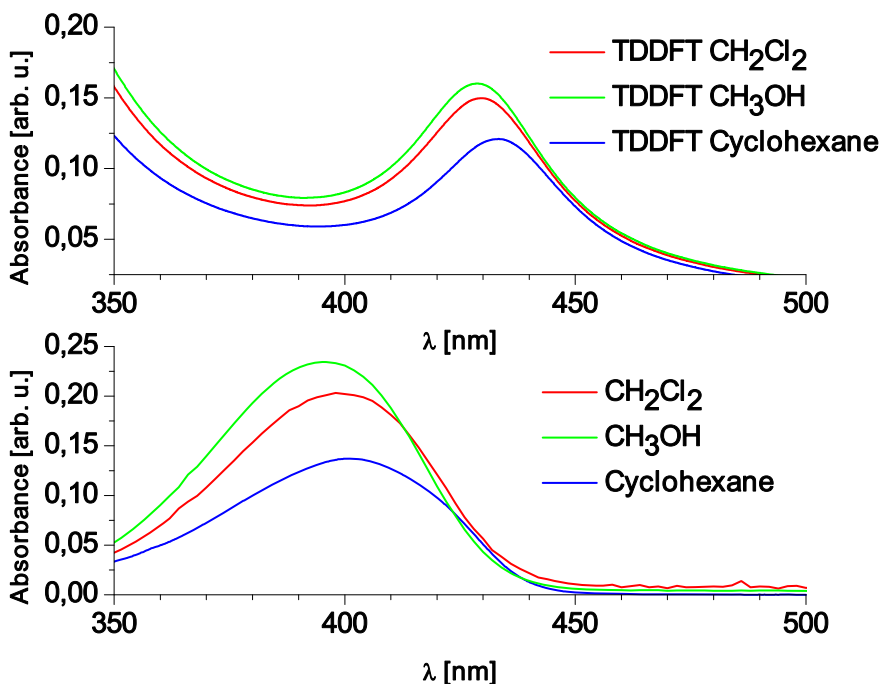


Figure 16. Solvatochromic effect in theoretical (top panel) and experimental (bottom) UV-vis absorption spectra of PQF1 manifested in the first absorption peak. The graphs are normalized to [0,1] interval.

The overall accuracy in UV-vis absorption spectra was very good in terms of both peak positions and relative intensities (PQF1, Figure 17). The spectra of other PQFs can be found in Publication III. The oscillator strengths, demonstrated in the spectra by the area under peaks and, to a lesser extent, peak height, were reproduced successfully in the computer simulation of the PQF materials, as can be seen in the figure. Thus, the TDDFT analysis was successful in reproducing both oscillator strength and transition frequencies.

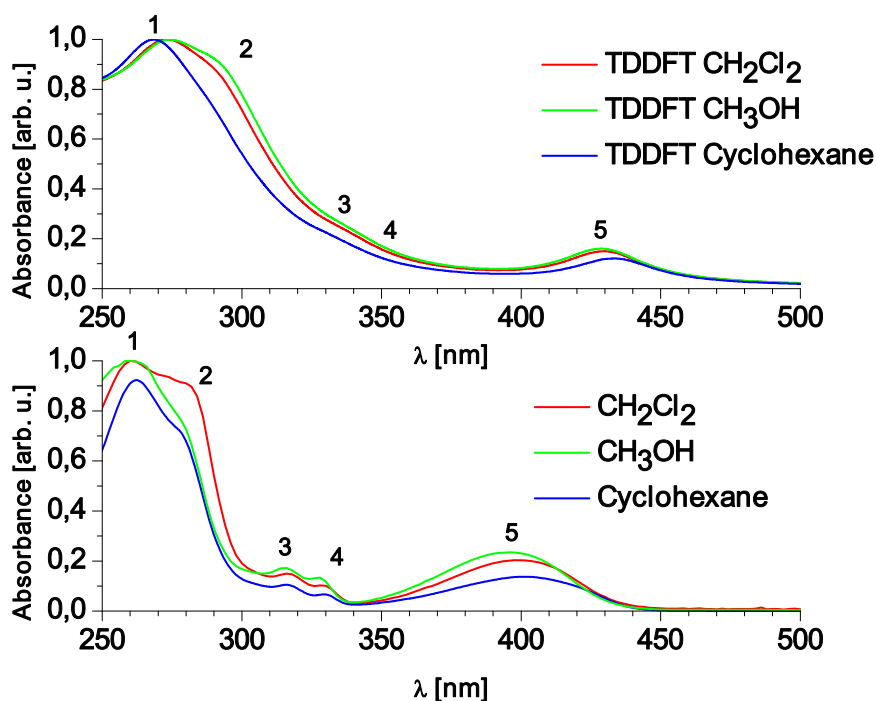


Figure 17. Complete theoretical (top panel) and experimental (bottom) UV-vis spectra of PQF1 in solvents of different polarity, demonstrating good agreement between simulated and empirical data on terms of peak intensities, positions and solvatochromic shift.

4.4. Conclusions

The performed combined experimental and theoretical studies of 1-(4-fluorophenyl)-3,4-diphenyl-1H-pyrazolo[3,4-b]quinoline, 3-(4-fluorophenyl)-1,4-diphenyl-1H-pyrazolo[3,4-b]quinoline and 4-(4-fluorophenyl)-1,3-diphenyl-1H-pyrazolo[3,4-b]quinoline have shown the chosen materials to be perspective for applications in Organic Light Emitting Diodes, electroluminescent displays and other photovoltaic devices. The main aim of such a combination was to get a deeper insight into the properties of the studied chromophores and establish a predictable trend for variation of these properties with varying environment.

Derivatives of pyrazoloquinoline containing fluorine atom have been described by computer modeling with a wide range of quantum-chemical methods, from Molecular Mechanics to Time-Dependent Density Functional Theory. The overall accuracy of theoretical predictions was good in both approaches: semi-empirical CIS simulation on MM+ optimized geometry and TDDFT simulation on DFT optimized molecules.

The semi-empirical methods reproduced the electronic structure and orbital energies to a satisfactory extent. The theoretical UV-vis spectra were in good agreement with the experimentally measured ones. Semi-empirical model PM3

underestimated energy gap in all the three PQF chromophores by 41 nm (experimental maximum of PQF1 at 396 nm/ 3.13 eV, PM3 at 437 nm/ 2.84 eV), while the AM1 and more recent RM1 methods both accurately described the first electronic transition (maxima at 404 and 414 nm, respectively). There is no significant improvement in RM1 performance over the AM1 model. Apparently, the error was caused by the computational method itself, not by the parameters it uses, and that is why re-parametrization in RM1 did not improve the calculation performance.

The interactions of the PQF molecules with environment have been described by the PCM solvation model. Four different solvents of different polarity were chosen as representative group of external matrices. Even though the changes of equilibrium geometries were minimal, the use of solvation models significantly changed the dipole moments of the molecules. The interaction with solvents changed TDDFT-derived UV-vis absorption spectra as well, leading to 4 nm blue shift of the first absorption peak in polar methanol in comparison with non-polar cyclohexane (maxima at 429 and 433 nm, respectively). Experimental data confirm theoretical results, with the blue shift almost identical in magnitude (5 nm, 396 to 401 nm). Apart from the red shift of the first absorption peak, the TDDFT-derived absorption spectra closely resemble experimental ones.

It seems reasonable to conclude that the solvation models should be included into the computational procedure whenever a strong interaction of the molecule with environment is expected. In this particular case, common solvents were used to model environmental influence on the studied molecules, but in principle the Polarizable Continuum Model can be applied to describe any dielectric medium, including polymers. The only parameter that has to be known is the dielectric constant of the matrix, which can be easily estimated from the polymer's dielectric constant. Thus, the quantum-chemical computer simulations including a solvation model can be used to simulate PQ chromophore properties in polymer matrices, which is precisely that environment in which they will be placed in practical applications.

5. QUANTUM-CHEMICAL DESCRIPTION OF DICYANOPYRAZINE-BASED CHROMOPHORES (III)

5.1.Aim

The main purpose of this research was to establish the structure-property relationship in a series of new X-shaped NLO-phores based on dicyanopyrazine (Figure 18, Figure 19). The central part of all the molecules is a pyrazine ring substituted with two cyano groups which strongly withdraw electrons and the electron-donating group is terminated with a 4-dimethylaminophenyl moiety. The varying part is the π -linker which consists of a phynyl ring(s) or phenyl ring(s) and ethynylene bridges. Thus, the X-shaped dicyanopyrazine derivatives' structure is characteristic to that of D- π -A (electron donor – π -linker – electron acceptor) NLO-phores and it is reasonable to expect them to undergo Intramolecular Charge Transfer (ICT) phenomena.

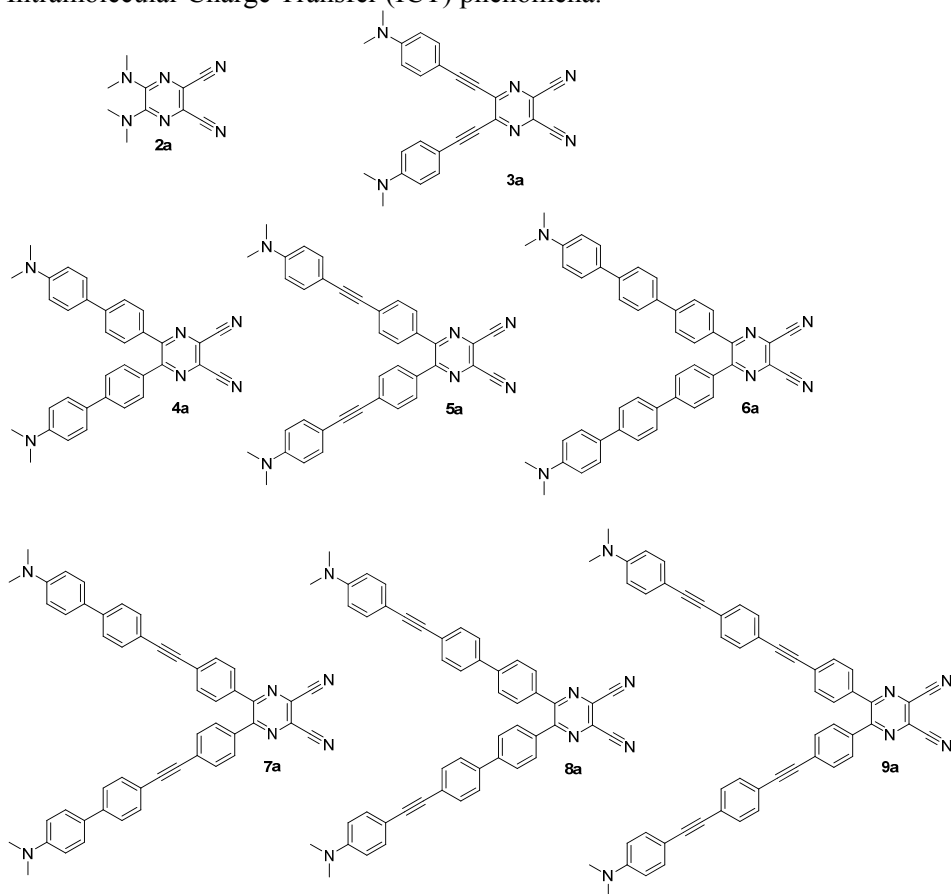


Figure 1. The “a” subseries of dicyanopyrazine chromophores.

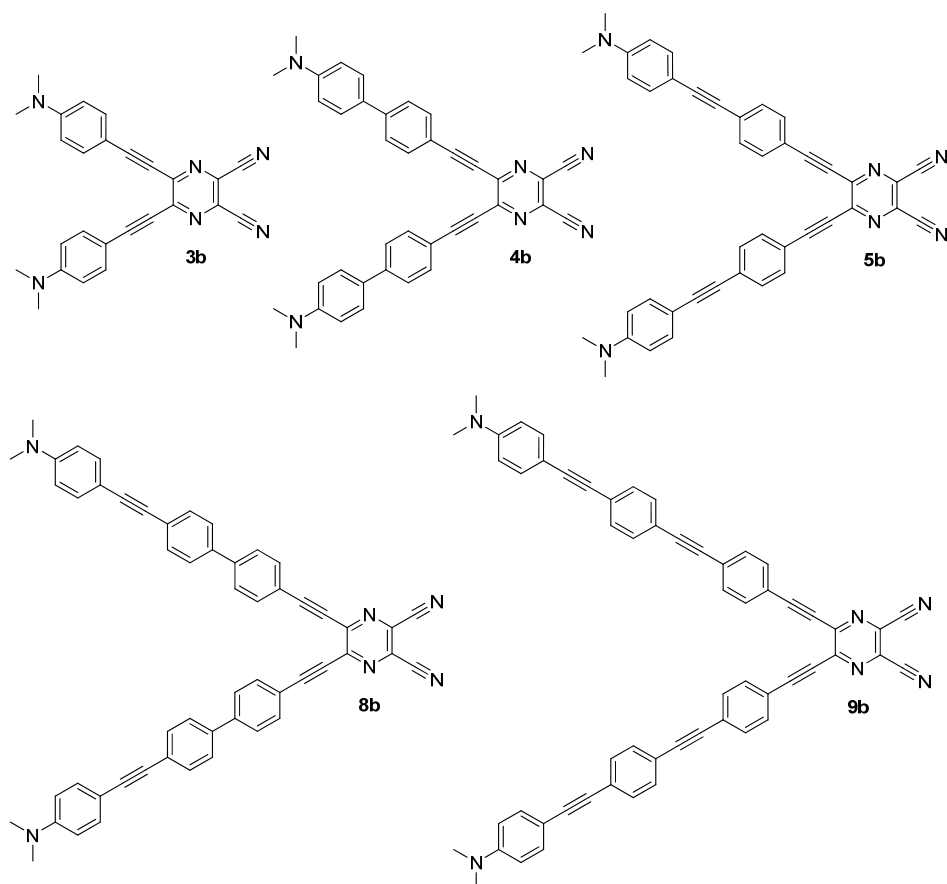


Figure 19. The “b” series of dicyanopyrazine chromophores.

In addition to synthesis description, the substances were characterized by crystallography, Cyclic Voltammetry, UV-vis absorption spectrometry and Second Harmonic Generation (SHG) experiments. The quantum-chemical calculations were used to aid experimental data interpretation and help formulate the conclusions. Computer simulations of the dicyanopyrazine NLO-phores covered equilibrium geometry, orbital energy levels and second order frequency-dependent hyperpolarizability $\beta(-2\omega, \omega, \omega)$, corresponding to generation of doubled-frequency light in the optically active material.

5.2. Methods

A semi-empirical method AM1 was chosen for calculations of the title molecules, due to its well-established reliability in performing organic molecule simulations, as well as low computational cost. In addition to the calculations

presented in Publication III, the following chapter contains results of DFT calculations, performed in BLYP/6-31++G(d,p) basis set containing both polarization and diffuse functions.

5.3. Results

The equilibrium geometry of the dicyanopyrazine based NLO-phores was established with the AM1 method. When compared with crystallographical data, it can be seen that the AM1-derived structures show good agreement with experiment in terms of the bond lengths and angles between them. However, it failed to reproduce the dihedral angles properly (Figure 20). They have been simulated correctly with the DFT method, but at substantially higher computational cost -optimization of relatively small compound 3a took 46 minutes at semi-empirical level of theory compared to 10 days 17 hours at DFT starting from AM1-optimized geometry using a 12-processor computational node with 21 GB of RAM memory. This discrepancy in dihedral angles probably affected the calculation accuracy, but the error was repeated in the whole series of simulated compounds and as a result the tendencies along the series were reproduced with satisfactory precision. Obviously, the increased ring rotation inhibited orbital delocalization similarly to twisted dihedral angle yielding good results (Figure 21).

The energy gap values interpreted as difference between HOMO and LUMO levels read from AM1 calculations are unreasonably high (6 to 8 eV instead of 1.4 to 2), which is typical for semi-empirical calculation. The trend along the series of compounds is, on the other hand, clearly reproduced in the quantum chemical calculations with high accuracy (Figure 23), with linear fit R^2 coefficient equal to 0.94. Evidently, the quantum-chemical AM1 simulation results allow one to compare other orbital properties along the series of studied dicyanopyrazine derivatives, such as shape and localization of the orbitals.

The main parameter of NLO-phores is their nonlinear susceptibility. In theoretical description the ability of a chromophore to exhibit NLO properties is reflected by the second and third order frequency-dependent polarizabilities, which can be found from Time-Dependent Hartree-Fock equations. In the studied dicyanopyrazine series the theoretical simulations showed a clear structure-property relationship consistent with the earlier research. Molecules with larger side substituents have higher value of $\beta(-2\omega, \omega, \omega)$, especially if the substituents are connected to the central dicyanopyrazine unit by a triple bond, ensuring planarity facilitating charge transfer. The theoretically predicted values were confirmed by experimental data, with linear fit coefficient R^2 equal to 0.83 (Figure 22).

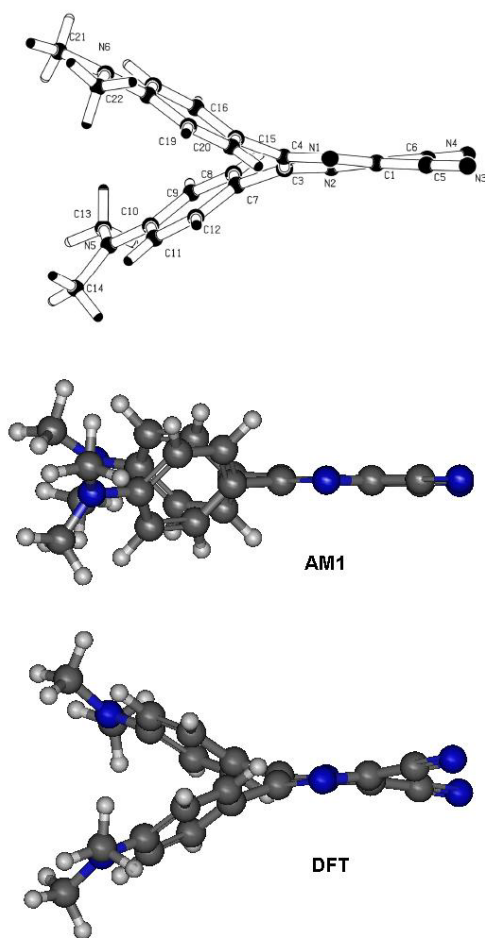


Figure 20. Experimental (top), AM1 and DFT BLYP/6-31++G(d,p) equilibrium geometries of compound 3a. The dihedral angles between pyrazine part and side substituents are not reproduced properly by the AM1 model.

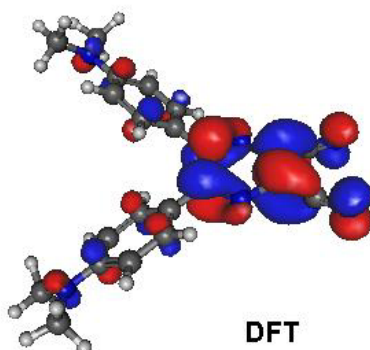
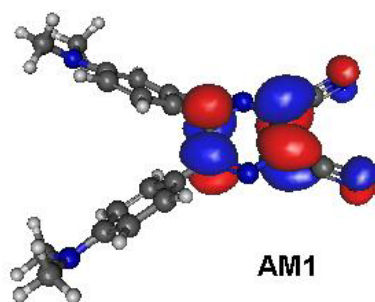


Figure 21. Visualization of LUMO orbital from AM1 and DFT BLYP/6-31++G(d,p) calculations. Orbital delocalization is similar in both cases, even though the dihedral angles differ as demonstrated in Figure 20.

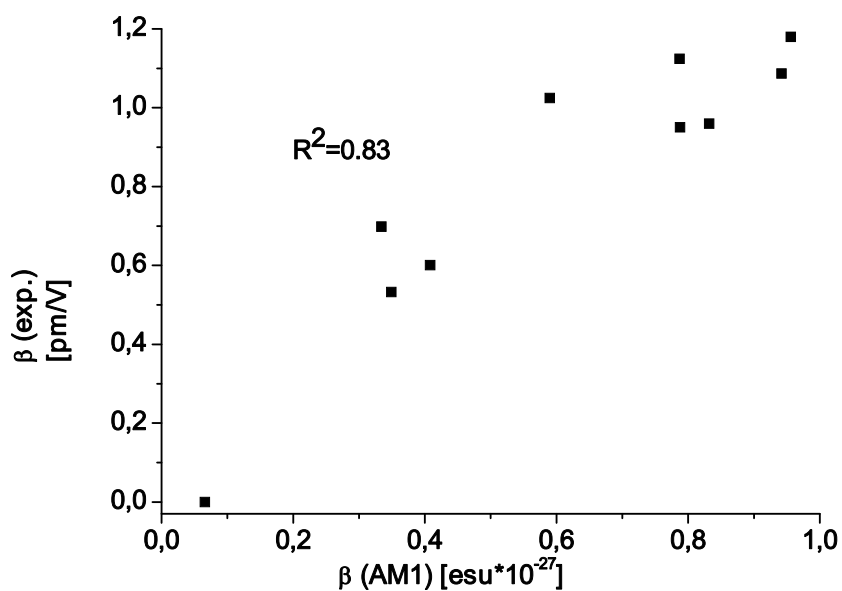


Figure 22. Correlation between experimental and theoretical second order dynamic hyperpolarizability.

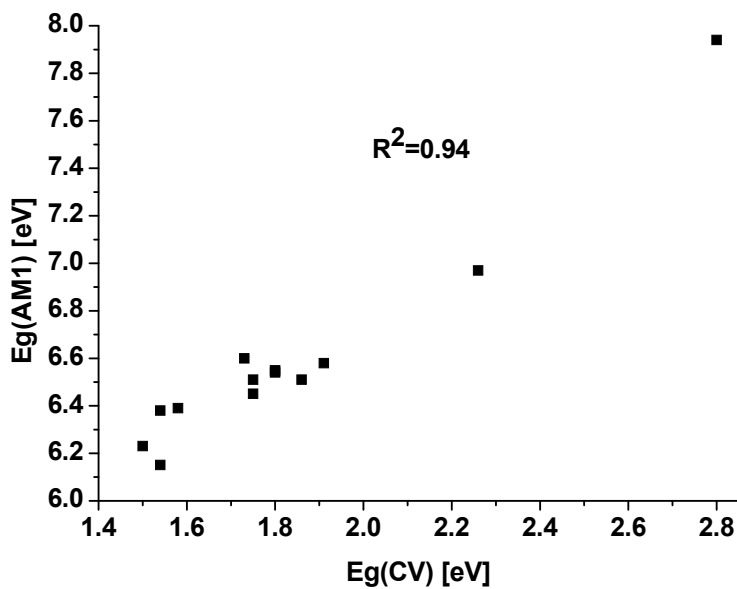


Figure 23. Correlation between experimental and theoretical energy gap.

5.4. Conclusions

The series of dicyanopyrazine-based NLO-phores were described with semi-empirical AM1 method. The simulation covered equilibrium geometry, electronic energy levels as well as second order dynamic hyperpolarizability, $\beta(-2\omega, \omega, \omega)$, which is a parameter describing NLO properties of the molecules. Theoretically derived values correlate well with experimental data, both in the case of Energy Gap (linear fit coefficient 0.94) and hyperpolarizability (0.83). The computer modelling confirmed structure-property relationship of the push-pull chromophores. Second order susceptibility was found to be dependent on π -linker and side substituent, serving as the electron donating group. The NLO response of the chromophore was found to be significantly larger if a triple bond was introduced to connect the π -linker and the pyrazine-2,3-dicarbonitrile. This relationship was found in the quantum-chemically simulated data as well. The aforementioned triple bonds render a more planar equilibrium geometry, which facilitates Donor-Acceptor conjugation and, as a result, improves Intramolecular Charge Transfer of the ground state in the molecules.

Thus, it can be concluded that the quantum-chemical computer simulations described the studied charge-transfer materials yielding satisfactory agreement with experimental data. Moreover, as the methods prove useful and accurate in predicting the dicyanopyrazine derivatives properties, they can be used in “virtual experiments”: in early design stage new materials can be subjected to quantum-chemical simulations and from a large set of new (in fact, so far non-existent) chromophores several most promising can be chosen for synthesis and further work.

6. SUMMARY

The quantum-chemical computer simulations have been successfully used to aid material design of the studied groups of optically active substances. Pyrazoloquinoline derivatives containing fluorine atom, a promising branch of luminescent molecules with potential application in LEDs and other electroluminescent devices, have been subjected to Molecular Mechanics, semi-empirical and DFT analysis (Publication I). Molecular geometry, energy levels and electronic transition energies have been described by theoretical simulations and the results are consistent with the corresponding experimental data. Semi-empirical Configuration Interaction simulation accurately reproduced excited states and optical transitions. In the studied pyrazoloquinoline derivatives the PM3 model underestimated the energy gap by 41 (first absorption maximum at 437 nm against experimental 396 nm), while the AM1 and RM1 simulations were more accurate. No significant improvement in RM1 results were observed in comparison with its predecessor, AM1.

In practical applications chromophores are almost never used in pure form. Typically they are placed in a transparent matrix, like a solvent or polymeric material. The matrix influences the chromophore and its optical properties and it is important to take that into account during new material design. Density Functional Theory models implemented in quantum-chemical packages can use solvation models to account for environmental influence on the studied molecules. In this work Polarizable Continuum Model was proven to be a very effective method to incorporate solvation effects in theoretical description of pyrazoloquinoline derivatives containing fluorine atom (Publication II). The choice of common solvents of different polarity as model matrices enabled facile experimental confirmation of the calculated solvatochromic effect. The environment's influence on optical properties of pyrazoloquinoline fluoro-derivatives was rather small, but well within the detection range (5 nm difference in the first absorption peak maximum) and it was correctly reproduced by TDDFT/PCM simulations. It is reasonable to predict that PCM will also be effective in the case of polymeric matrices and in prediction of higher order hyperpolarizabilities in future research.

Computer simulations have been successfully applied to theoretically describe the NLO response in a series of dicyanopyrazine derivatives belonging to the push-pull chromophore group. Molecular structure is known to significantly influence the nonlinear optical properties of the material. As it was demonstrated in Publication III, the π -linker connecting the electron-donating and electron-accepting groups can play crucial role in the intramolecular charge transfer process, especially if it ensures planarity of the equilibrium molecular geometry. The theoretically derived second order dynamic hyperpolarizabilities correlated very well with experimental data from the Second Harmonic Generation measurement. Energy gaps calculated from the HOMO and LUMO

difference also correlated very well with the empirical data obtained from a cyclic voltammetry oxidation and reduction peaks.

Computational chemistry methods have proven to be a useful tool in all the cases presented in this work. As such, they can be used to aid design of new optically active materials in future research in the field of both linear and non-linear optics. Additionally, incorporation of solvation models into DFT and TDDFT calculations can be used to predict matrix influence on optical properties of the embedded chromophores which can prove very useful in practical applications.

7. SUMMARY IN ESTONIAN

Väitekirja raames teostatud töö eesmärgiks oli kahe perspektiivse kromofooride rühma, *pyrazoloquinoline* ja *dicyanopyrazine* derivaatide optiliste omaduste teoreetilise kirjelduse andmine. Nimetatud ainetele on viimase 15 aasta jooksul osutatud märkimisväärset tähelepanu tänu nende võrdlemisi lihtsale sünteesile, hästi-defineeritud struktuurile, keemilisele ja termilisele stabiilsusele ning võimalusele nende omadusi timmida molekulaarse struktuuri modifitseerimise teel. Neile leidub võimalikke rakendusi optoelektronika seadmetes, orgaanilistes valgusdiodides (OLED), päikesepatareides, optilistes lülites, andmesalvestusseadmetes ja mujal. Kirjanduses on demonstreeritud mitmete seadmete prototüüpe. Selleks et teoreetiliselt kirjeldada uuritud kromofooride optilisi omadusi, valiti rida poolempiirilisi ja DFT meetodeid, mis pakusid mõistliku kompromissi arvutuskiiruse ja täpsuse vahel.

Kvantkeemia arvutisimulatsioone on edukalt kasutatud uuritud ainete rühma baasil optiliselt aktiivsete materjalide disainimiseks. Molekulaardünaamika, poolempiirilise ja DFT analüüsi abil on uuritud fluori sisaldavaid *pyrazoloquinoline* derivaate, mis võiksid omada potentsiaalset rakendust valgusdiodides jm elektroluminestsentsseadmetes (publikatsioon I). Teoreetilistest simulatsioonidest on leitud molekuli tuumakonfiguratsioonid, energiatasemed ja elektronüleminekute energiad ja tulemused on kooskõlas vastavate eksperimentaalsete andmetega. Poolempiirilise, konfiguratsioonide vastasmõju arvestava simulatsiooniga oli võimalik suure täpsusega reprodutseerida ergastatud olekud ja optilised üleminekud. Uuritud *pyrazoloquinoline* derivaatide korral PM3 mudel alahindas energiapilu 41 nm võrra (esimene neeldumismaksimum 437 nm võrrelduna eksperimentaalse väärtusega 396 nm) samas kui AM1 ja RM1 simulatsioonid olid täpsemad. RM1 tulemused ei olnud oluliselt paremad võrreldes tema eelkäijaga AM1.

Praktilistes rakendustes ei kasutata kromofoore peaaegu kunagi puhtal kujul. Tüüpiliselt on nad asetatud läbipaistvasse maatriksisse nagu lahusti või polümeer. Maatriks avaldab mõju kromofoori optilistele omadustele ja seda tuleb uute materjalide disainimisel arvesse võtta. Tiheduse funktsionaalteooria (DFT) mudelid, mis leiduvad kvantkeemia programmpakettides, suudavad solvendiefektide kaudu arvesse võtta ka ümbruse mõju uuritavale molekulile. Selles näidati, et polariseeruva kontiinumi mudel (PCM) on väga efektiivne meetod solvendiefektide arvestamiseks fluori sisaldavate *pyrazoloquinoline* derivaatide teoreetilisel kirjeldamisel (publikatsioon II). Mitmesuguste erineva polaarsusega laialt levinud lahustite kasutamine mudelainetena võimaldas lihtsasti realseerida arvatud solvatokroomiliste efektide eksperimentaalset kinnitust. Leiti, et ümbruse mõju *pyrazoloquinoline* fluoroderivaatidele on üsna väike kuid kindlalt detekteeritav (5 nm erinevus esimese piigi asukohas) ja seda oli võimalik korrektselt reprodutseerida TDDFT/PCM simulatsioonidega. On mõistlik eeldada, et PCM on efektiivne ka polümeermaatriksite korral ja kõrgemat järku hüperpolariseeritavuste arvutamisel tulevastest uuringutes.

Arvutisimulatsioone on edukalt rakendatud ka *dicyanopyrazine* derivaatide rühma kuuluvate kromofooride mittelineaarse optilise koste kirjeldamisel. On teada, et molekulaarne struktuur mõjutab märkimisväärselt materjali mittelineaarseid optilisi omadusi. Publikatsioonis III demonstreeritakse, et π -side, mis ühendab elektron-doonor ja elektron-aktseptor rühmi, mängib otsustavat rolli molekulisisesel laenguülekandeprotsessil, eriti kui ta vastutab molekuli tasakaalulise geomeetria tasapinnalisuse eest. Teoreetiliselt leitud teist järku dünaamiline hüperpolariseeritavus korreleerub väga hästi teise harmooniku genereerimise eksperimentaalsete andmetega. Energiapilud, mis on arvutatud HOMO ja LUMO erinevuse põhjal, korreleeruvad samuti väga hästi empiiriliste andmetega, mis on saadud tsüklilise voltampermeetriaga oksüdatsiooni ja reduktsiooni piikidel.

Arvutuskeemia meetodid on osutunud kasulikeks vahenditeks kõigi käesolevas väitekirjas esitatud juhtudel. Sel viisil saab neid kasutada suunamaks uute optiliste materjalide disaini tulevastes uuringutes nii lineaarse kui ka mittelineaarse optika vallas. Lisaks, solvendimudelite kaasamine DFT ja TDDFT arvutustesse võimaldab ennustada maatriksi mõju lisandkromofooridele, mis võib osutuda väga kasulikuks praktilistes rakendustes.

8. REFERENCES

1. G. Diestrau, *Journal de Chem. Phys. et Physico-Chemie Boil.* **33** (1936) 620.
2. C. W. Tang, S. A. Van Slyke, *Appl. Phys. Lett.* **51** (1987) 913.
3. E. Gondek, I. V. Kityk, A. Danel, *Mater. Chem. Phys.* **112** (2008) 301.
4. D. M. Burland, R. D. Miller, O. Reiser, R. J. Twieg, C. A. Walsh, *J. Appl. Phys.* **71** (1992) 410.
5. G. Zhang, C. B. Musgrave *J. Phys. Chem. A* **111** (2007) 1554.
6. A. Musierowicz, S. Niementowski, Z. Tomasik, *Rocz. Chem.* **8** (1928) 325.
7. Z. He, G. H. W. Milburn, A. Danel, A. Puchala, P. Tomasik, D. Rasala, *J. Mater. Chem.* **7** (1997) 2323.
8. A. Danel, Z. He, G. H. W. Milburn, P. Tomasik, *J. Mater. Chem.* **9** (1999) 339.
9. K. Rechthaler, K. Rotkiewicz, A. Danel, P. Tomasik, K. Katchatrian, G. Kohler, *J. Fluoresc.* **7** (1997) 301.
10. A. B. J. Parusel, K. Rechhaaler, D. Piorun, A. Danel, K. Khatchatryan, G. Kohler, *J. Fluoresc.* **8** (1998) 375.
11. L. Mu, Z. He, J. Wang, G. Hui, Y. Wang, X. Jing, A. Danel, E. Kulig, *IEEE Photon. Technol. Lett.* **20** (2008) 1781.
12. J. Nizol, A. Danel, G. Boiteux, J. Davenas, B. Jarosz, A. Wisla, G. Seytre, *Synth. Met.* **127** (2002) 175.
13. M. G. Kuzyk, *J. Mater. Chem.* **19** (2009) 7444.
14. W. Cornell, P. Cieplak, C. I. Bayly, I. R. Gould, K. M. Merz, D. M. Ferguson, D. C. Spellmeyer, T. Fox, J. W. Caldwell, P. A. Kollman, *J. Am. Chem. Soc.* **117** (1995) 5179.
15. M. D. Wodrich, C. Corminboeuf, P. R. Schreiner, A. A. Fokin, P. von Ragué Schleyer, *Org. Lett.* **9** (2007) 1851.
16. W. Koch, M. C. Holthausen, *A Chemist's Guide to Density Functional Theory*, Wiley-VCH Verlag GmbH ISBNs: 3-527-60004-3 (Electronic)
17. A. Szabo, N. S. Ostlund, *Modern Quantum Chemistry: Introduction to Advanced Electronic Structure Theory*, MacMillan Publishing Co., New York, 1982.
18. M. Born, J. R. Oppenheimer, *Ann. Physik* **84** (1927) 458.
19. MM+ is based on MM2 forcefield, N. L. Allinger, *J. Am. Chem. Soc.* **99** (1977) 8127.
20. S. W. Tkaczyk, I. V. Kityk, R. Schiffer, *J. Phys. D: Appl. Phys.* **35** (2002) 563.
21. E. Hückel, *Zeitschrift für Physik* **70** (1931) 204; **72** (1931) 310; **76** (1932) 628; **83** (1933) 632.
22. A. Streitwieser, *Molecular Orbital Theory for Organic Chemists*, Wiley, New York, 1961.
23. R. Hoffmann, *J. Chem. Phys.* **39** (1963) 1397.
24. M. J. S. Dewar, E. Zebisch, E. F. Healy, J. J. P. Stewart, *J. Am. Chem. Soc.* **107** (1985) 3902.
25. J. J. P. Stewart, *J. Comp. Chem.* **10** (1989) 209.
26. G. B. Rocha, R. O. Freire, A. M. Simas, J. J. P. Stewart, *J. Comp. Chem.* **27** (2006) 1101.
27. R. C. Bingham, M. J. S. Dewar, D. H. Lo, *J. Am. Chem. Soc.* **97** (1975) 1285.
28. M. J. S. Dewar, W. Thiel, *J. Am. Chem. Soc.* **99** (1977) 4899.
29. P. Hohenberg, W. Kohn, *Phys. Rev.* **136** (1964) B864.

30. W. Kohn, L. J. Sham, *Phys. Rev.* **140** (1965) A1133.
31. M. E. Casida, Time Dependent Density Functional Response Theory for Molecules, Recent Advances in Density Functional Methods, Part I, Chong, D. P. (ed.), World Scientific, Singapore, 1995.
32. S. Miertus, E. Scrocco, J. Tomasi, *Chem. Physics* **55** (1981) 117.
33. S. Miertus, J. Tomasi, *Chem. Physics* **65** (1982) 239.
34. G. Scalmani, M. J. Frisch, B. Mennucci, J. Tomasi, R. Cammi, V. Barone, *J. Chem. Phys.* **124** (2006) 1.
35. R. McWeeny, *Rev. Mod. Phys.* **32** (1960) 335.
36. R. McWeeny, *Phys. Rev.* **126** (1962) 1028.
37. P. Pulay, *J. Chem. Phys.* **78** (1983) 5043.
38. C. E. Dykstra, P. G. Jasien, *Chem. Phys. Lett.* **109** (1984) 388.
39. HyperChem(TM) Professional 8.04, Hypercube, Inc., 1115 NW 4th Street, Gainesville, Florida 32601, USA
40. Gaussian 09, Revision A.02, M. J. Frisch, G. W. Trucks, H. B. Schlegel, G. E. Scuseria, M. A. Robb, J. R. Cheeseman, G. Scalmani, V. Barone, B. Mennucci, G. A. Petersson, H. Nakatsuji, M. Caricato, X. Li, H. P. Hratchian, A. F. Izmaylov, J. Bloino, G. Zheng, J. L. Sonnenberg, M. Hada, M. Ehara, K. Toyota, R. Fukuda, J. Hasegawa, M. Ishida, T. Nakajima, Y. Honda, O. Kitao, H. Nakai, T. Vreven, J. A. Montgomery, Jr., J. E. Peralta, F. Ogliaro, M. Bearpark, J. J. Heyd, E. Brothers, K. N. Kudin, V. N. Staroverov, R. Kobayashi, J. Normand, K. Raghavachari, A. Rendell, J. C. Burant, S. S. Iyengar, J. Tomasi, M. Cossi, N. Rega, J. M. Millam, M. Klene, J. E. Knox, J. B. Cross, V. Bakken, C. Adamo, J. Jaramillo, R. Gomperts, R. E. Stratmann, O. Yazyev, A. J. Austin, R. Cammi, C. Pomelli, J. W. Ochterski, R. L. Martin, K. Morokuma, V. G. Zakrzewski, G. A. Voth, P. Salvador, J. J. Dannenberg, S. Dapprich, A. D. Daniels, O. Farkas, J. B. Foresman, J. V. Ortiz, J. Cioslowski, and D. J. Fox, Gaussian, Inc., Wallingford CT, 2009.
41. J. B. Foresman, M. Head-Gordon, J. A. Pople, M. J. Frisch, *J. Phys. Chem.* **96** (1992) 135.
42. R. Bauernschmitt, R. Ahlrichs, *Chem. Phys. Lett.* **256** (1996) 454.
43. A. A. Granovsky, Firefly 7.1.G, <http://classic.chem.msu.su/gran/firefly/index.html>
44. M. W. Schmidt, K. K. Baldridge, J. A. Boatz, S. T. Elbert, M. S. Gordon, J. H. Jensen, S. Koseki, N. Matsunaga, K. A. Nguyen, S. Su, T. L. Windus, M. Dupuis, J. A. Montgomery, *J. Comput. Chem.* **14** (1993) 1347.
45. A. R. Allouche, Gabedit is a free Graphical User Interface for computational chemistry packages. It is available from <http://gabedit.sourceforge.net/>
46. C. J. Cramer, Essentials Of Computational Chemistry, John Wiley & Sons Ltd, ISBN 0-470-09181-9, 2004.

ACKNOWLEDGEMENTS

I would like to thank my supervisor, Prof. Mikhail Brik, for his support and involvement in preparation of this thesis. Were it not for his continuous help and advice, this thesis would not have been prepared.

I am thankful to Prof. Ivan Kityk, who has introduced me to the realm of computational chemistry and tutored me for the past four years.

Would also like to thank Dr. Valter Kiisk for his help with writing the Estonian language parts of this thesis.

I would like to thank my family for their understanding and patience in times when research work separated me from them.

A large part of the quantum-chemical calculations presented in this thesis has been carried out in the Wroclaw Centre for Networking and Supercomputing, <http://www.wcss.wroc.pl> (grant number 135).

The research presented in this thesis was supported by European Social Fund's Doctoral Studies and Internationalisation Programme DoRa.

PUBLICATIONS

CURRICULUM VITAE

Wojciech Kuznik

Date and place of birth: April 22, 1985, Czestochowa, Poland
Citizenship: Polish
Address: Kokoszeki 2/46, 44–100 Gliwice, Poland
E-mail: wojtek.kuznik@gmail.com

Education

1999–2003 Liceum im. Adama Mickiewicza w Lublincu
2003–2008 Silesian University of Technology, Faculty of Chemistry
specialization: Technology and Engineering of Fine Chemicals and
Specialty Materials, MSc. In Chemical Technology
2008– PhD Studies, Silesian University of Technology, Faculty of
Chemistry, discipline: Chemistry

Scientific work

Main fields of research: computational chemistry of optically active systems
Publications: 15 scientific articles

Teaching experience

Physics, Physical Chemistry – laboratory practice, 2004–2011, Silesian University of Technology, Faculty of Chemistry, 300 hours in total

Awards

2007/08 Ministry of Science and Higher Education Scholarship for student excellence, Poland

CURRICULUM VITAE IN ESTONIAN

Wojciech Kuznik

Sünniaeg ja koht: 22.aprill 1985, Czestochowa, Poola
Kodakondsus: Poola
Aadress: Kokoszki 2/46, 44–100 Gliwice, Poola
E-mail: wojtek.kuznik@gmail.com

Haridustee

1999–2003 Adam Mickiewicz Gümnaasium, Lubliniec
2003–2008 Sileesia Tehnoloogiaülikool, Keemia Teaduskond
spetsialiseerumine: erimaterjalide valmistamise tehnoloogia
2008– doktorant, Sileesia Techniline Ülikool, Keemia Teaduskond
spetsialiseerumine: keemia,

Teadustegevus

Peamine töösuund: Optiliselt aktiivsete süsteemide arvutuskeemia
Publikatsioonid: 15 teaduslikku publikatsiooni

Õpetöö kogemus

Füüsika, Füüsikalise Keemia – praktikum, 2004–2011, Sileesia Tehnoloogia-
ülikool, Keemia Teaduskond, kokku 300 tundi

Erialane tunnustus

2007/08 Poola Teaduse ja Kõrghariduse Ministeeriumi stipendium välja-
paistvale üliõpilasele

DISSERTATIONES SCIENTIAE MATERIALIS UNIVERSITATIS TARTUENSIS

1. **Martin Järvekülg.** Tubular microstructures by Hf-, Zr- and Ti-butoxide gel sheet rolling. Tartu, 2011, 112 p.
2. **Sergei Vlassov.** Investigation of nanoscale interactions and mechanical properties of nanostructures using quartz tuning fork based real-time measurements. Tartu, 2011, 171 p.
3. **Margus Kodu.** Pulsed Laser Deposition of Magnesium Oxide and Barium Ternary Oxides for Plasma Display Protective Layers. Tartu, 2011, 89 p.
4. **Rainer Pärna.** Surface studies of some oxide films. Tartu, 2011, 129 p.
5. **Jevgeni Šulga.** Self-assembly and interaction of nanostructures. Tartu, 2011, 114 p.